asthma (17–19), pulmonary fibrosis (20), myocardial infarction (21), valvular heart disease (22), cystic fibrosis (23) and proliferative diabetic retinopathy (24). Further, it has been shown that the biological functions of periostin as a matricellular protein rather than structural player are important for the pathogenesis of some of these diseases. For instance, periostin affects eosinophils and/or epithelial cells in bronchial asthma, enhancing eosinophil migration and/or activating TGF-β, respectively (25,26). Moreover, in the healing process of myocardial infarction, periostin may enhance cardiac repair via stimulation of myocyte proliferation (27), although whether this is a direct mechanism or via adjacent cardiac fibroblasts remains controversial (28). Furthermore, periostin accelerates the development of various tumors by promoting cancer cell survival, epithelial–mesenchymal transition, invasion and metastasis (29,30). In contrast, the physiological roles of periostin remain poorly understood, except for several studies using periostin-deficient mice that suggest non-replaceable roles for periostin during development of bone, tooth and heart valves (14,31).

Importantly for this study, periostin is known to be highly expressed in wounds, suggesting its involvement in the process of wound repair (32,33). To directly examine the role of periostin within the process of cutaneous wound repair, we employed both *in vivo* and *in vitro* approaches using systemic periostin-deficient mice, exogenous periostin supplementation and a well-characterized mouse wound repair model. Significantly, wound repair is delayed in periostin-deficient mice. Furthermore, exogenous periostin up-regulates proliferation and migration of the dermal fibroblasts, which suggests this may be the mechanism how periostin accelerates cutaneous wound repair. These results demonstrate that periostin is required for the process of cutaneous wound repair, highlighting its physiological role, and suggest that periostin may be a useful candidate to therapeutically speedup wound repair.

Methods

Mice

Eight- to twelve-week-old C57BL/6 or BALB/c mice (Japan SLC, Japan), periostin-deficient (*Postn*$^{-/-}$, C57BL/6 or BALB/c background) mice, were used (14,21). Experiments were undertaken following the guidelines for care and use of experimental animals required by the Japanese Association for Laboratory Animals Science (1987).

Mouse wound repair model

Mice were anaesthetized by inhalation of halothane or intraperitoneal injection of pentobarbital. After their backs were shaved, 8- or 10-mm diameter full-thickness wounds were generated using disposable biopsy punches (Kai Industries, Seki, Japan). Wound sizes were measured longitudinally with a slide calliper. Wound tissues were excised at indicated time points postinjury and used for quantitative RT-PCR, Western blotting or histological analysis. Following fixation in 3.7% formaldehyde and embedding in paraffin, histological analysis was performed on serial sections from spanning the central portion of the wound and stained with haematoxylin and eosin (H&E), Masson's trichrome and/or via immunohistochemical staining as previously described (18,20). In selected experiments, 2 μg recombinant mouse periostin (R&D Systems, Minneapolis, MN, USA) was painted onto the wound lesions every 2 days from day 1 to 9.

Quantitative RT-PCR

Quantitative RT-PCR was used to measure periostin as previously described (18). Briefly, RNA from wound site was isolated using an RNeasy Mini kit (Qiagen Japan, Tokyo, Japan), and the RT reaction was performed using a QuantiTect Reverse Transcription Kit (Qiagen Japan). Quantitative analysis was achieved using Applied Biosystems StepOnePlus™ Real-Time PCR System (Life Technologies Japan, Tokyo, Japan). The primer sequence and PCR conditions are referred to the Data S1.

Confocal microscopy

Excised wound tissues were fixed with 3.7% formaldehyde and embedded in paraffin. After blocking with 2% BSA, the wax sections were stained using polyclonal anti-periostin Ab, previously prepared (18) followed by Alexa488-labelled anti-rabbit IgG Ab (Invitrogen, Carlsbad, CA, USA). The sections were mounted by Dako fluorescent mounting medium (Dako, Glostrup, Denmark) and then examined by LSM5 PASCAL G/B microscope (Carl Zeiss Japan, Tokyo, Japan).

Transduction of periostin into MEFs

Mouse full-length *Postn* cDNA was cloned (ENSMUST000000-81564) from MEF. Overexpression of mouse periostin into wild-type or periostin-deficient MEFs was performed using retroviral transduction of pMXs-puro vector [provided by Dr. Toshio Kitamura, Tokyo University, Tokyo, Japan (34)]. As a control, an empty vector was used alongside periostin-containing vector. After transduction, only infected cells were selected by 1 μg/ml puromycin (InvivoGen, San Diego, CA, USA).

Proliferation assay

Proliferation of fibroblasts was examined using the Cell Counting Reagent SF (Nacalai Tesque, Kyoto, Japan) according to the manufacturer's recommendations. In selected experiments, after 4-h serum starvation, dermal fibroblasts were seeded on the specified concentration of recombinant periostin (as described previously).

Statistical analyses

The results are presented as means + SD. Analysis was carried out using the two-sided, unpaired Student's *t*-test or the two-sided Welch test. Multiple comparisons between groups were performed by Fisher's or Dunnett's methods. We considered values to be significant when $P < 0.05$.

Results

Periostin expression is induced in wound tissues

We first analysed the expression of periostin in wound tissues. In C57BL/6 mice, periostin mRNA started to increase at day 1 after injury and peaked at day 7, decreasing thereafter (Fig. 1a, $n = 8$). Correspondingly, periostin protein levels peaked at day 7–10 and were sustained until day 18 (Fig. 1b). Wounded mice on the BALB/c background showed almost identical kinetics of periostin temporal changes at both the mRNA and protein levels (Fig. S1, $n = 8$). We then examined whether the localization of periostin was altered in wounded tissues. In the normal unwounded skin, periostin was expressed weakly at the dermal–epidermal junction and relatively robustly around the hair follicles (Figs 1c and S2). At day 6, when the wound was still open with hypertrophic epidermal wound edges and granulation tissues formed beneath these edges, periostin was now strongly expressed in the dermal–epidermal junction at these edges and within the granulation tissues. At day 9, when the wound was closed, significant expression of periostin was still observed in the granulation tissues beneath

© 2012 John Wiley & Sons A/S, *Experimental Dermatology*

COLOR

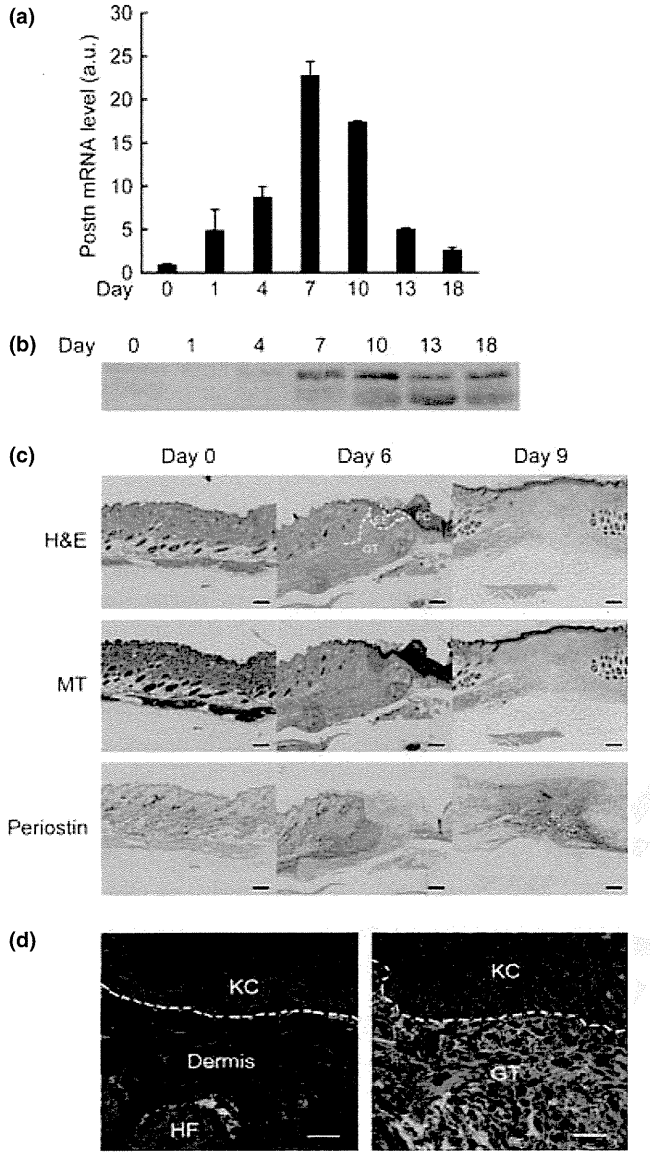

Figure 1. Periostin expression in wounded tissues. (a, b) Analysis of expression of periostin mRNA (a) or periostin protein (b) in wounded skin of C57BL/6 (n = 8) mice following the indicated amount of days postinjury. In b, experiments were repeated three times, and the representative combined data are depicted. (c) Wound sites stained with H&E, Masson trichrome (MT) and anti-periostin Ab from wild-type C57BL/6 mice for the indicated amount of days postinjury. FC, fibrin clot; EE, epidermal edge; GT, granulation tissue. Scale bar represents 200 μm. (d) Confocal microscopic imaging of wounds at day 6 is shown. Left and right panels depict non-wounded or wounded areas, respectively. Green and red represent periostin and the intrinsic fluorescence of cells, respectively. Scale bar represents 20 μm. KC, keratinocyte; GT, granulation tissue; HC, hair follicle.

the re-epithelialized wounds. To assess localization, we double-stained periostin (appears green), and this enabled us to conclude that periostin was deposited only at the border between the epidermis and the dermis and around hair follicles in the non-wounded sites, whereas periostin was deposited in the interspace regions of the red-staining granulation tissues in the wounded sites (Fig. 1d). These results demonstrate that periostin is induced during wound repair, suggesting that periostin may play a role in the repair process as well as being a useful marker of well-organized wound repair.

Periostin is required for efficient wound repair in mice

To test the functional requirement of periostin in wound repair, we used periostin-deficient ($Postn^{-/-}$) mice to perform wounding and assess their response. The wound sizes during the healing time course were significantly reduced in $Postn^{+/+}$ mice in C57BL/6 background (Fig. 2a,b, n = 10 for each genotype, $P < 0.05$ at day 3, 5 and 11, $P < 0.01$ at day 7) and in $Postn^{+/-}$ mice in a BALB/c background (Fig. S3, n = 3 for $Postn^{-/-}$ and n = 6 for $Postn^{+/-}$, $P < 0.05$ at day 3 and 10, $P < 0.001$ at day 13) than those observed in age-matched litter $Postn^{-/-}$ mice. Accordingly, the time intervals to completely close the wounds were significantly extended in $Postn^{-/-}$ mice than within $Postn^{+/+}$ mice (Fig. S4, 14.1 ± 0.74 days vs 15.9 ± 1.6 days, $P < 0.05$).

When we painted recombinant periostin protein onto the wounded area of $Postn^{-/-}$ mice every 2 days, starting day 1 after injury to day 9, the observed slower wound repair was subsequently accelerated (Fig. 2c,d upper panel, n = 10 for each group, the wound sizes: $P < 0.01$ at day 3, $P < 0.001$ at day 5 and 7, the time interval required to close the wounds: 15.9 ± 1.6 days vs 13.8 ± 1.4 days, $P < 0.01$). Moreover, the effects of administering exogenous periostin on accelerating wound repair were observed even in $Postn^{+/+}$ mice (Fig. 2c lower panel and Fig. S4, the wound sizes: $P < 0.05$ at day 7, the time interval to close the wounds: 14.1 ± 0.74 days vs 12.8 ± 1.1 days, $P < 0.01$). Thus, these results clearly demonstrate the requirement and positive effect of periostin within the wound repair process in mice.

Effect of periostin on proliferation in dermal fibroblasts

It has been shown that periostin can bind $\alpha_v\beta_3$ and $\alpha_v\beta_5$ integrin heterodimers (13,14) and that signalling via integrin molecules is imperative for cell proliferation and migration (10–12). Thus, we confirmed that α_v, β_3 and β_5 integrins, but not β_4 integrin, were expressed in human dermal fibroblasts, although A431 cells express β_4 integrin (Fig. S5A). Furthermore, when we stimulated human dermal fibroblasts with recombinant periostin, phosphorylation of downstream molecules of integrins focal adhesion kinase [FAK, STAT3, Akt and p44/42MAPK] was also observed (Fig. S5B). These results suggest that the interaction of periostin with human dermal fibroblasts is able to activate key signalling pathways via integrins present in the wound.

The present observation that periostin was strongly deposited within the granulation tissues beneath the hypertrophic epidermal wound edges raised the possibility that periostin may directly affect fibroblast proliferation, thereby accelerating the repair process. To explore this possibility, we initially examined the effects of exogenous periostin on proliferation of normal human dermal fibroblasts (NHDFs). We confirmed that NHDFs proliferate in response to FGF2 (Fig. S6). We also found that proliferation of NHDFs was up-regulated in a dose-dependent manner of periostin coated on plates (Fig. 3a, $P < 0.05$ at periostin 0.1 μg/ml, 24 h, $P < 0.01$ at periostin 1 μg/ml, 24 h, $P < 0.001$ at periostin 0.1 or 1 μg/ml, 72 h and at periostin 0.1 or 1 μg/ml, 120 h). We then analysed the effects of periostin deficiency on proliferative activities of mouse dermal fibroblasts. Fibroblast cultures established from skin of newborn $Postn^{-/-}$ mice had impaired proliferation compared with fibroblasts from $Postn^{+/+}$ mice (Fig. 3b, $P < 0.05$ at 6 and 48 h, $P < 0.01$ at 24 h, $P < 0.001$ at 72 h). Treatment

with recombinant periostin slightly enhanced proliferation of fibroblasts from both wild-type (Fig. 3c, $P < 0.05$ at 72 h) and periostin-deficient ($P < 0.05$ at 12 and 24 h) mice. Further, we overexpressed retrovirally periostin in periostin-deficient fibroblasts and in wild-type fibroblasts (Fig. S7). As expected, these periostin-overexpressed cells had significantly up-regulated proliferation compared with mock-transfected wild-type (Fig. 3d, $P < 0.001$ at 24, 48, 60 and 72 h) or periostin-deficient (Fig. 3d, $P < 0.01$ at 60 and 72 h, $P < 0.001$ at 24 and 48 h) fibroblasts, respectively. These *in vitro* data demonstrate that either exogenously added or ectopically expressed periostin enhances the proliferative activities of fibroblasts.

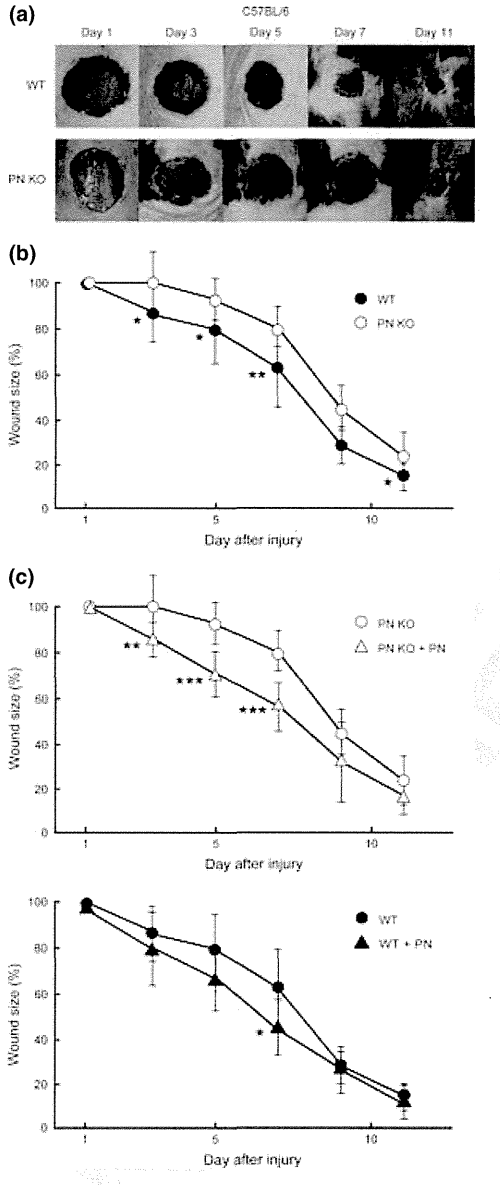

Figure 2. Periostin is important for efficient wound healing in mice. Successive photographs of the wounds (a), wound sizes at the indicated amount of days postinjury (b) in wild-type (WT, $n = 10$), or periostin-deficient mice (PN KO, $n = 10$) in C57BL/6 background. (c) Recombinant human periostin (+PN 2 μg) was injected intradermally into wounds of C57BL/6 background mice ($n = 10$ for each of WT and PN KO) every 2 days, from day 1 after injury to day 9. Wound sizes at the indicated times after injury (c). Statistical differences between PN KO vs WT, PN KO + PN vs PN KO and WT + PN vs WT are depicted. $*P < 0.05$, $**P < 0.01$, $***P < 0.001$.

Periostin enhances migration of dermal fibroblasts

We then examined the effects of periostin on migration of dermal fibroblasts using scratch wound cell monolayer method in wild-type and periostin-deficient MEFs (Fig. 4a,b). To exclude confounding effects upon proliferation, we arrested cell growth prior to analysis of migration. We confirmed that the migration activity of wild-type MEFs was up-regulated by platelet-derived growth factor (PDGF), whereas that was down-regulated by cytochalasin D (Fig. S8). The motility of periostin-deficient MEFs was significantly impaired compared with that of wild-type MEFs ($P < 0.05$ at 24 h). These results demonstrate that periostin can also enhance migration as well as the proliferation status of fibroblasts in response to wounding.

Discussion

It is well recognized that the ECM regulates the functions of the various cell lineages mobilized to the wounded area, contributing not only to re-epithelialization but also to granulation tissue formation and angiogenesis (35). Moreover, several studies using genetically deficient mice have shown that ECM proteins can play important *in vivo* functions during wounding and repair. For instance, fibronectin and its co-receptor, syndecan-4, are thought to accelerate wound repair as loss-of-function mouse mutants defective in the extra domain A of fibronectin or syndecan-4 both exhibit delayed cutaneous wound repair (36,37), whereas thrombospondin-1 and -2 play an opposite role and mainly inhibit wound repair (38,39). Based on previous observations that periostin is an ECM protein highly expressed during wound repair in various mouse models (32,33), in this study, we used periostin-deficient mice to test its requirement via our wound repair model. Meaningfully, both *in vivo* and *in vitro* results support the conclusion that periostin accelerates the wound healing process. Recently, using periostin-deficient mice, Nishiyama et al. (40) also reported that lack of periostin delays the process of cutaneous wound repair. Taking these results together, the requirement of periostin for the process of efficient cutaneous wound repair is well established.

The Nishiyama et al. (40) data indicated that periostin up-regulates keratinocyte proliferation and migration, accelerating the process of re-epithelialization. This result is consistent with our observation of significant periostin expression observed in the dermal–epidermal junction during wound repair. In our study, we similarly demonstrate that periostin enhances proliferation and migration of fibroblasts, which would contribute to the process of granulation tissue formation. We also demonstrated that periostin is deposited in fibroblast-enriched granulation tissues. Fibroblasts contribute to wound repair by generating several growth factors important for re-epithelialization (8) and by differentiating into α-SMA-expressing myofibroblasts important to close the wound edges by TGF-β1 (1–4). Collectively, these suggest that periostin deposition and the formation of fibroblast-enriched granulation tissues is the critical step during wound repair. The significance of fibroblast activation during wound repair is also supported by data from profibrotic cytokine, FGF2-null mice (41). Therefore, it is likely that direct or indirect activation of dermal fibroblasts by presence of periostin may be an additional mechanism underlying

© 2012 John Wiley & Sons A/S, *Experimental Dermatology*

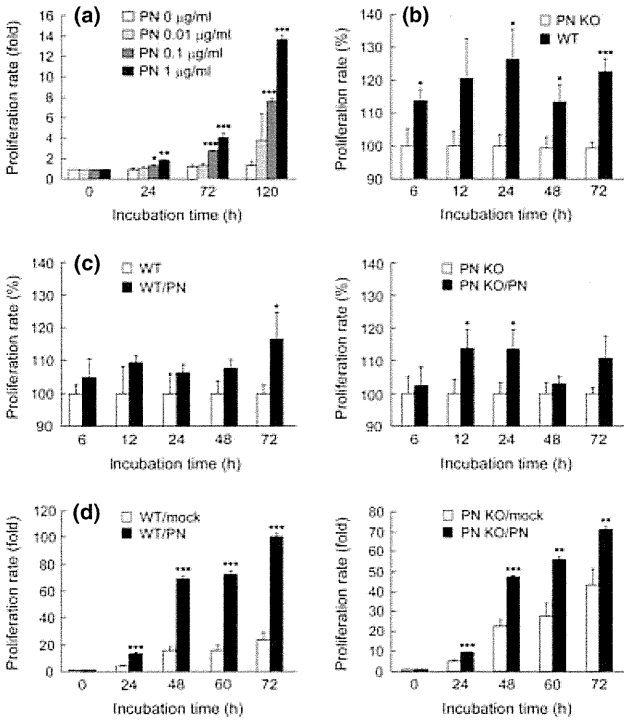

Figure 3. Effects of periostin on fibroblast proliferation. (a–c) Normal human dermal fibroblasts (a) or mouse dermal fibroblasts derived from wild-type (WT) or periostin-deficient mice (PN KO) (b, c) were cultured for various times. In panel (a), the concentrations of human periostin used are indicated, and in panel (c), 100 ng/ml of mouse periostin was used to coat the culture dishes. (d) Mouse periostin-overexpressed or mock-transduced MEFs (3×10^3 cells) derived from wild-type (WT) or periostin-deficient (PN KO) mice were cultured for various lengths. The proliferation rate was estimated using the Cell Counting Reagent SF. The relative folds were compared with the starting points (a, d) or PN KO-type or to fibroblasts on non-coated plates (b, c) are depicted. In panel (a), one-way ANOVA followed by Dunnett's test was used for multiple comparisons of the different fibroblast rates induced by various concentrations of periostin. Statistical differences were compared with PN 0 ng/ml cultures. Experiments were repeated five times, and the representative combined data are depicted. $*P < 0.05$, $**P < 0.01$, $***P < 0.001$.

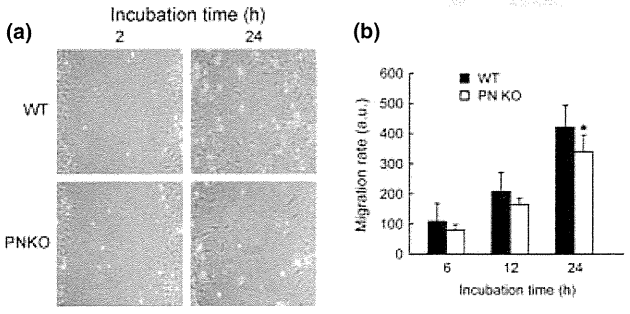

Figure 4. Effects of periostin on the migration of fibroblasts. Analysis of cell migration in MEFs derived from wild-type (WT) or periostin-deficient (PN KO) mice were compared. Photographs of the wounded cell monolayers at 2 and 24 h (a) and the relative cell motilities at various times indicated (b). The average cell motility (14 points per one field and three different fields/well in triplicate) was calculated and shown. Statistical difference between WT vs PN KO ($*P < 0.05$) is depicted.

wound repair, in addition to periostin activation of keratinocytes (40).

It is well known that TGF-β1 is highly expressed in wounded tissues and can act as a central enhancer of wound repair effectors (42,43). Consequently, mice deficient in TGF-β1 show delayed cutaneous wound repair (44). When we examined whether TGF-β1 or other cytokines were able to directly induce periostin expression in human dermal fibroblasts and accumulated periostin in the supernatant was seen in responses to IL-4 and IL-13 (17,18) and to TGF-β1, whereas several other cytokines (IL-1β, -6, -17, tumor necrosis factor-α, FGF-2, FGF-5, stromal cell-derived factor-1, and PDGF) were not able to induce periostin expression (Fig. S9). Collectively, these results suggest that TGF-β1, abundant in the wound site, mainly contributes to periostin induction and that induction of periostin is a novel biological function of TGF-β1 within the well-ordered process of wound repair.

Targeted genetic deletion of periostin in mice significantly impairs fibroblast proliferation and wound healing, whereas fibroblast proliferation and wound healing can be enhanced by exogenous periostin, suggesting a direct role for periostin. Furthermore, treatment of dermal fibroblasts with exogenous periostin activates integrin-associated signalling molecules (FAK, STAT3, Akt and p44/42MAPK). As integrin-mediated signalling is initiated by formation of the Src/FAK complex, which enhances cell proliferation by up-regulating cyclin D1 expression via p44/42MAPK or cell survival by inhibiting proapoptotic factors such as Bad, caspase nine, forkhead transcription factors via PI3K/Akt (10–12), our results indicate that several levels of the proliferation pathway are activated when periostin is present. Moreover, STAT3 transduces signals important for cell proliferation and survival, cooperating with growth factor receptor-mediated signals (45,46). Periostin has been shown to induce proliferation of smooth muscle and/or cancer cells via the FAK/PI3K/Akt pathway (47,48). In contrast, genetic inhibition or administration of MAPK inhibitors delays wound repair (49,50). Finally, direct activation of the PI3K/Akt pathway is known to accelerate wound repair (51). These collective results suggest that periostin–integrins signal via FAK, STAT3, Akt and p44/42MAPK and play an important role in wound repair via augmenting cell proliferation/survival.

Clinically, it may be imperative to modulate either delayed (e.g. from diabetes or radiation exposure) or enhanced wound repair [e.g. hypertrophic and keloid scars (2,3)]. However, disappointing clinical results from single-agent therapies such as administering growth factors or other mediators to boost wound repair suggest that it is a highly ordered and complex process. Our surprising result, that injection of periostin into the wound in mice models can accelerate the healing process, may suggest that topical administration of periostin could be efficacious in wound treatment. Furthermore, it is now hoped that recent advances in stem cell/progenitor cell biology and material sciences will make it possible to entirely replace tissues. Our present data regarding the role of periostin in wound repair indicate that it could be a useful addition in construction of optimized skin tissues.

In conclusion, in this study, we demonstrate that periostin, transiently expressed during wound repair, accelerates the process by activating dermal fibroblasts. Although the pathological roles of periostin within fibrosis in various diseases have recently been well characterized, the physiological roles of periostin in skin repair are starting to be uncovered. Our present study demonstrates a novel physiological role for periostin: namely, its involvement in effective cutaneous wound repair.

© 2012 John Wiley & Sons A/S, *Experimental Dermatology*

Acknowledgements

We thank Dr. Dovie R. Wylie, Hiroyuki Ideguchi, Yumiko Ohishi, Yukako Kanazawa and Maiko Urase for critical review of this manuscript, technical and secretarial assistance. KO, YK, HS, SS and LY performed the research. AT, MF, YN, HM, ST, IK, KI and TN designed the research study. SO, KA, SS, AK and SJC contributed essential reagents or tools. KO, YK, SJC and KI wrote the paper. This work was supported in part by Grants-in-Aid for Scientific Research from the Japan Society for the Promotion of Science and by Grant-in-Aid from the Ministry of Health, Labour and Welfare, Japan.

Conflict of interests

The authors have no declared no conflicts of interests.

References

1 Baum C L, Arpey C J. Dermatol Surg 2005: **31**: 674–686.
2 Gurtner G C, Werner S, Barrandon Y *et al.* Nature 2008: **453**: 314–321.
3 Singer A J, Clark R A. N Engl J Med 1999: **341**: 738–746.
4 Palatinus J A, Rhett J M, Gourdie R G. J Mol Cell Cardiol 2010: **48**: 550–557.
5 Ranzato E, Martinotti S, Volante A *et al.* Exp Dermatol 2011: **20**: 308–313.
6 Kim J H, Jung M, Kim H S *et al.* Exp Dermatol 2011: **20**: 383–387.
7 Novotny M, Vasilenko T, Varinska L *et al.* Exp Dermatol 2011: **20**: 703–708.
8 Werner S, Grose R. Physiol Rev 2003: **83**: 835–870.
9 Desmouliere A, Geinoz A, Gabbiani F *et al.* J Cell Biol 1993: **122**: 103–111.
10 Eliceiri B P. Circ Res 2001: **89**: 1104–1110.
11 Giancotti F G, Ruoslahti E. Science 1999: **285**: 1028–1032.
12 Hynes R O. Trends Cell Biol 1999: **9**: M33–M37.
13 Hamilton D W. J Cell Commun Signal 2008: **2**: 9–17.
14 Rios H, Koushik S V, Wang H *et al.* Mol Cell Biol 2005: **25**: 11131–11144.
15 Midwood K, Sacre S, Piccinini A M *et al.* Nat Med 2009: **15**: 774–780.
16 Shinohara M L, Kim J H, Garcia V A *et al.* Immunity 2008: **29**: 68–78.
17 Hayashi N, Yoshimoto T, Izuhara K *et al.* Proc Natl Acad Sci U S A 2007: **104**: 14765–14770.
18 Takayama G, Arima K, Kanaji T *et al.* J Allergy Clin Immunol 2006: **118**: 98–104.
19 Woodruff P G, Boushey H A, Dolganov G M *et al.* Proc Natl Acad Sci U S A 2007: **104**: 15858–15863.
20 Okamoto M, Hoshino T, Kitasato Y *et al.* Eur Respir J 2011: **37**: 1119–1127.
21 Shimazaki M, Nakamura K, Kii I *et al.* J Exp Med 2008: **205**: 295–303.
22 Hakuno D, Kimura N, Yoshioka M *et al.* J Clin Invest 2010: **120**: 2292–2306.
23 Oku E, Kanaji T, Takata Y *et al.* Int J Hematol 2008: **88**: 57–63.
24 Yoshida S, Ishikawa K, Asato R *et al.* Invest Ophthalmol Vis Sci 2011: **52**: 5670–5678.
25 Blanchard C, Mingler M K, McBride M *et al.* Mucosal Immunol 2008: **1**: 289–296.
26 Sidhu S S, Yuan S, Innes A L *et al.* Proc Natl Acad Sci U S A 2010: **107**: 14170–14175.
27 Kuhn B, del Monte F, Hajjar R J *et al.* Nat Med 2007: **13**: 962–969.
28 Lorts A, Schwanekamp J A, Elrod J W *et al.* Circ Res 2009: **104**: e1–e7.
29 Fujimoto K, Kawaguchi T, Nakashima O *et al.* Oncol Rep 2011: **25**: 1211–1216.
30 Ruan K, Bao S, Ouyang G. Cell Mol Life Sci 2009: **66**: 2219–2230.
31 Snider P, Hinton R B, Moreno-Rodriguez R A *et al.* Circ Res 2008: **102**: 752–760.
32 Jackson-Boeters L, Wen W, Hamilton D W. J Cell Commun Signal 2009: **3**: 125–133.
33 Zhou H M, Wang J, Elliott C *et al.* J Cell Commun Signal 2010: **4**: 99–107.
34 Kitamura T, Koshino Y, Shibata F *et al.* Exp Hematol 2003: **31**: 1007–1014.
35 Midwood K S, Williams L V, Schwarzbauer J E. Int J Biochem Cell Biol 2004: **36**: 1031–1037.
36 Echtermeyer F, Streit M, Wilcox-Adelman S *et al.* J Clin Invest 2001: **107**: R9–R14.
37 Muro A F, Chauhan A K, Gajovic S *et al.* J Cell Biol 2003: **162**: 149–160.
38 Kyriakides T R, Tam J W, Bornstein P. J Invest Dermatol 1999: **113**: 782–787.
39 Streit M, Velasco P, Riccardi L *et al.* EMBO J 2000: **19**: 3272–3282.
40 Nishiyama T, Kii I, Kashima T G *et al.* PLoS One 2011: **6**: e18410.
41 Ortega S, Ittmann M, Tsang S H *et al.* Proc Natl Acad Sci U S A 1998: **95**: 5672–5677.
42 Barrientos S, Stojadinovic O, Golinko M S *et al.* Wound Repair Regen 2008: **16**: 585–601.
43 Werner S, Krieg T, Smola H. J Invest Dermatol 2007: **127**: 998–1008.
44 Crowe M J, Doetschman T, Greenhalgh D G. J Invest Dermatol 2000: **115**: 3–11.
45 Guo W, Pylayeva Y, Pepe A *et al.* Cell 2006: **126**: 489–502.
46 Shin H D, Park B L, Kim L H *et al.* Hum Mol Genet 2004: **13**: 397–403.
47 Bao S, Ouyang G, Bai X *et al.* Cancer Cell 2004: **5**: 329–339.
48 Li G, Jin R, Norris R A *et al.* Atherosclerosis 2010: **208**: 358–365.
49 Sharma G D, He J, Bazan H E. J Biol Chem 2003: **278**: 21989–21997.
50 Thuraisingam T, Xu Y Z, Eadie K *et al.* J Invest Dermatol 2010: **130**: 278–286.
51 Lai J P, Dalton J T, Knoell D L. Br J Pharmacol 2007: **152**: 1172–1184.

Supporting Information

Additional Supporting Information may be found in the online version of this article:

Figure S1. Periostin expression in wounded tissues.

Figure S2. Expression of periostin in the wound sites in mice.

Figure S3. Periostin is important for efficient wound healing in mice.

Figure S4. Periostin is important for efficient wound healing in mice.

Figure S5. Activation of human dermal fibroblasts by exogenous periostin.

Figure S6. Effects of fibroblast growth factor-2 on fibroblast proliferation.

Figure S7. Establishment of periostin-transduced MEFs.

Figure S8. Effects of cytochalasin D and platelet-derived growth factor on cell migration.

Figure S9. Analysis of periostin responses in human dermal fibroblasts to various stimuli.

Data S1. Materials and methods.

Please note: Wiley-Blackwell is not responsible for the content or functionality of any supporting materials supplied by the authors. Any queries (other than missing material) should be directed to the corresponding author for the article.

© 2012 John Wiley & Sons A/S, *Experimental Dermatology*

ORIGINAL ARTICLE

Serum Leucine-rich Alpha-2 Glycoprotein Is a Disease Activity Biomarker in Ulcerative Colitis

Satoshi Serada, PhD, Minoru Fujimoto, MD, PhD,* Fumitaka Terabe, MD, PhD,*† Hideki Iijima, MD, PhD,† Shinichiro Shinzaki, MD, PhD,† Shinya Matsuzaki, MD,‡ Tomoharu Ohkawara, MD,* Riichiro Nezu, MD, PhD,§ Sachiko Nakajima, MD, PhD,† Taku Kobayashi, MD, PhD,‖ Scott Eric Plevy, MD, PhD,‖ Tetsuo Takehara, MD, PhD,† and Tetsuji Naka, MD, PhD**

Background: Reliable biomarkers for monitoring disease activity have not been clinically established in ulcerative colitis (UC). This study aimed to investigate whether levels of serum leucine-rich alpha-2 glycoprotein (LRG), identified recently as a potential disease activity marker in Crohn's disease and rheumatoid arthritis, correlate with disease activity in UC.

Methods: Serum LRG concentrations were determined by enzyme-linked immunosorbent assay (ELISA) in patients with UC and healthy controls (HC) and were evaluated for correlation with disease activity. Expression of LRG in inflamed colonic tissues from patients with UC was analyzed by western blotting and immunohistochemistry. Interleukin (IL)-6-independent induction of LRG was investigated using IL-6-deficient mice by lipopolysaccharide (LPS)-mediated acute inflammation and dextran sodium sulfate (DSS)-induced colitis.

Results: Serum LRG concentrations were significantly elevated in active UC patients compared with patients in remission ($P < 0.0001$) and HC ($P < 0.0001$) and were correlated with disease activity in UC better than C-reactive protein (CRP). Expression of LRG was increased in inflamed colonic tissues in UC. Tumor necrosis factor alpha (TNF-α), IL-6, and IL-22, serum levels of which were elevated in patients with active UC, could induce LRG expression in COLO205 cells. Serum LRG levels were increased in IL-6-deficient mice with LPS-mediated acute inflammation and DSS-induced colitis.

Conclusions: Serum LRG concentrations correlate well with disease activity in UC. LRG induction is robust in inflamed colons and is likely to involve an IL-6-independent pathway. Serum LRG is thus a novel serum biomarker for monitoring disease activity in UC and is a promising surrogate for CRP.

(Inflamm Bowel Dis 2012;000:000–000)

Key Words: IBD, ulcerative colitis, biomarker, leucine-rich alpha-2 glycoprotein, DSS

The chronic inflammatory bowel diseases (IBDs), Crohn's disease (CD) and ulcerative colitis (UC), are typically characterized by episodes of acute flares and remission.[1,2] Depending on disease location and extent, exacerbation leads to diarrhea, abdominal pain, and systemic symptoms such as fatigue and weight loss.[3–5] Disease activity indices have been developed as outcome measures in clinical trials.[6,7] They may help to reproducibly and validly assess the patients' status and to support therapeutic decision-making.[6] Variables of disease activity indices comprise frequency of bowel movements, severity of abdominal pain, general well-being, occurrence of extra-intestinal manifestations, and laboratory parameters.[8]

One of the most important protein biomarkers increased during the inflammatory state is C-reactive protein (CRP). However, elevation of serum CRP levels is not observed in certain inflammatory diseases. While serum CRP levels are highly increased in CD and rheumatoid arthritis (RA) patients and widely used for monitoring

Additional Supporting Information may be found in the online version of this article.

Received for publication February 12, 2012; Accepted February 13, 2012.

From the *Laboratory for Immune Signal, National Institute of Biomedical Innovation, Osaka, Japan, †Department of Gastroenterology and Hepatology, Osaka University Graduate School of Medicine, Osaka, Japan, ‡Department of Obstetrics and Gynecology, Osaka University Graduate School of Medicine, Osaka, Japan, §Department of Surgery, Osaka Rosai Hospital, Osaka, Japan, ‖Center for Gastrointestinal Biology and Diseases, University of North Carolina School of Medicine, Chapel Hill, North Carolina, USA.

Supported by the Grant-in-Aid for Scientific Research (C) (22591101) from the Japanese Ministry of Education, Science, Sports, and Culture; a grant-in-aid for the Program for Promotion of Fundamental Studies in Health Sciences of the National Institute of Biomedical Innovation and Grant-in-Aid from the Ministry of Health, Labour and Welfare of Japan.

Reprints: Tetsuji Naka, Laboratory for Immune Signal, National Institute of Biomedical Innovation, 7-6-8, Saito-asagi, Ibaraki, Osaka 567-0085, Japan (e-mail: tnaka@nibio.go.jp).

Copyright © 2012 Crohn's & Colitis Foundation of America, Inc.

DOI 10.1002/ibd.22936

Published online in Wiley Online Library (wileyonlinelibrary.com).

TABLE 1. Characteristics of Patients with Ulcerative Colitis (UC)

Characteristics	Patients with UC	Patients with Appendicitis and Diverticulitis
Number (male:female)	82 (41:41)	17 (8:9)
Age, yr, mean (SD)	40.1 (15.7)	33.1 (13.7)
Age at diagnosis, yr, mean (SD)	34.7 (15.6)	33.1 (13.7)
Bowel surgery (including appendectomy), *N* (%)	7 (8.54)	
Treatment		
Salazosulfapyridine or mesalazine, N (%)	66 (80.5)	
Steroids, *N* (%)	16 (19.5)	
Immunomodulators, *N* (%)	3 (3.7)	
Disease location (*N*)		
Extensive colitis/left-sided colitis/proctitis	37/30/15	
CRP, mg/dL, mean (SD)	0.884 (1.967)	8.47 (7.69)
WBC cells/μl, mean (SD)	6716 (2317)	12307 (3603)
CAI, mean (SD)	4.71 (4.89)	
Matts's score, mean (SD)	2.27 (0.89)	

disease activity, only modest to absent CRP responses are observed in systemic lupus erythematosus (SLE), dermatomyositis, Sjogren's syndrome, or UC, although active inflammation is present.[9–11] In UC, endoscopic disease activity may predict future clinical symptoms,[12] but direct endoscopic or radiologic visualization of the degree of inflammation is rarely performed in outpatients with inactive or mild disease. Therefore, alternative biomarkers, which can conveniently and precisely monitor disease activity during therapy in inflammatory diseases, are required for the determination of adequate treatment.

By using a quantitative proteomic approach, we have previously reported that serum levels of leucine-rich alpha-2 glycoprotein (LRG) were elevated in patients with active RA and serum LRG levels were correlated with disease activity of not only RA but also CD, suggesting that serum LRG is a serological biomarker for monitoring disease activity.[13] LRG is an ≈50 kDa glycoprotein and contains repetitive sequences with a leucine-rich motif, first purified from human serum.[14,15] LRG has been reported to be expressed by the liver cells and neutrophils[16,17]; however, its function remains unclear. To date, the relationship between serum LRG levels and disease activity in UC has not been assessed. In this study we investigated serum LRG expression levels in UC patients and evaluated their correlation with clinical disease activity. Serum LRG levels were significantly increased in the active UC patients. LRG expression was upregulated in the inflamed colonic mucosa of UC possibly through stimulation by various cytokines including tumor necrosis factor alpha (TNF-α), interleukin (IL)-6, and IL-22, the expression of which are increased in active UC. Moreover, we show that serum LRG correlates more strongly than CRP with disease activity in UC. Therefore, serum LRG may be a useful disease activity biomarker for UC.

MATERIALS AND METHODS

Patients and Sera

Sera were obtained from patients with UC ($n = 82$), appendicitis ($n = 13$), and diverticulitis ($n = 4$) and surgical or biopsy samples were obtained from patients with UC ($n = 10$) from Osaka University Hospital (Osaka, Japan) and the Department of Surgery, Osaka Rosai Hospital, respectively. Sera from healthy controls (HCs) ($n = 50$), age/sex-matched with UC patients, were used. Diagnosis of UC was based on conventional clinical, radiological, endoscopic, and histopathological criteria. Clinical activities were determined using the Clinical Activity Index (CAI) for UC.[18] Clinical remission was defined as CAI <6.[19] In addition to CAI, the endoscopic findings were also graded according to Matts' criteria.[20] Endoscopic remission was defined as Matts' score ≤2. Detailed patient characteristics are presented in Table 1. For Caucasian patients with UC, sera ($n = 30$) were obtained from the Department of Medicine, University of North Carolina Hospital (Chapel Hill, NC). Sera from HCs ($n = 19$), age/sex-matched with UC patients, were used. Detailed patient characteristics are presented in Table 2, while data of disease activity of UC is not available.

Quantification of Serum LRG and Cytokines

Human serum LRG and mouse serum LRG were quantitated by human LRG assay kit (IBL, Fujioka, Japan) and mouse LRG assay kit (IBL, Fujioka, Japan). These enzyme-linked immunosorbent assay (ELISA) assays were performed

TABLE 2. Characteristics of Patients with UC in a Caucasian Cohort

Characteristics	Patients with UC
Number (male:female)	30 (18:12)
Age, yr, mean (SD)	42.9 (17.9)
Age at diagnosis, yr, mean (SD)	33.2 (15.7)
Treatment	
Salazosulfapyridine or mesalazine, *N* (%)	14 (46.7)
Steroids, *N* (%)	9 (30.0)
Immunomodulators, *N* (%)	11 (36.7)
Anti-TNF therapy	3 (10.0)
Disease location (*N*)	
Extensive colitis/left-sided colitis/proctitis	16/11/3

in duplicate. The intraassay coefficients of variations for human LRG and mouse LRG were $\leq$7.98% and $\leq$8.93%, respectively. For the quantification of IL-6, TNF-α, and IL-22 in human serum samples, the human IL-6 Ultra Sensitive ELISA (Biosource International, Camarillo, CA), human TNF-α UltraSensitive ELISA kit (Invitrogen, Carlsbad, CA), and human IL-22 Quantikine ELISA Kit (R&D Systems, Minneapolis, MN) were used following the manufacturer's guidelines.

Western Blot Analysis

Frozen colon tissue samples were lysed in RIPA buffer (10 mM Tris-HCl, pH 7.5, 150 mM NaCl, 1% Nonidet P-40, 0.1% sodium deoxycholate, 0.1% SDS, 1 × protease inhibitor cocktail; Nacalai Tesque, Kyoto, Japan) and 1 × phosphatase inhibitor cocktail (Nacalai Tesque) followed by centrifugation (13,200 rpm, 4°C, 15 minutes), after which the supernatants were stored at −80°C until use. Extracted proteins were subjected to sodium dodecyl sulfate-polyacrylamide gel electrophoresis (SDS-PAGE) as described previously.[21] Samples transferred onto PVDF membranes were treated with a rabbit antihuman LRG polyclonal antibody (Proteintech Group, Chicago, IL) or a rabbit anti-GAPDH polyclonal antibody (Santa Cruz Biotechnology, Santa Cruz, CA) was used as described previously.[21]

Immunohistochemistry

Immunohistochemical analyses were performed according to a method described in our previous report.[22] Briefly, rabbit antihuman LRG polyclonal antibodies were used as the primary antibody. After incubation with the primary antibodies, the sections were treated with biotin-conjugated goat anti-rabbit IgG (Vector Laboratories, Burlingame, CA) and avidin-biotin-peroxidase complexes (Vector Laboratories). Immunoreactive cells were visualized with a diaminobenzidine substrate (Merck, Darmstadt, Germany) and were counterstained with hematoxylin.

Mice

C57BL/6 mice were purchased from Clea Japan (Tokyo, Japan). C57BL/6-background IL-6-deficient mice were kindly provided by Professor Yoichiro Iwakura (Laboratory of Molecular Pathogenesis, Center for Experimental Medicine, Institute of Medical Science, University of Tokyo, Tokyo, Japan). Mice were maintained under specific pathogen-free conditions. C57BL/6 and IL-6-deficient mice were used at 7–9 weeks of age. All experiments were conducted according to the institutional ethical guidelines for animal experimentation.

LPS-mediated Acute Inflammation

To induce acute inflammation, wildtype (WT) mice and IL-6-deficient mice were injected intraperitoneally with 0 or 10 mg/kg LPS (*Escherichia coli* LPS, Sigma, St. Louis, MO) dissolved in 500 μL phosphate-buffered saline (PBS). Blood was collected at before and 24 hours after LPS injection and the serum was separated by centrifugation and stored at −30°C until used for ELISA analysis.

Induction of Colitis

For induction of colitis, WT mice and IL-6-deficient mice were given 3% dextran sodium sulfate (DSS) (m/w 36,000–50,000; MP Biomedicals, Solon, OH) dissolved in drinking water provided ad libitum for 5 days, followed by provision of ordinary water for 20 days.

Assessment of Severity of DSS-induced Colitis

WT mice were weighed daily from day 0 to day 25. Changes in body weight were calculated as follows: body weight change (%) = [(weight on a given day (days 0–13) − weight on day 0)/weight on day 0] * 100. Blood was collected from WT mice on days 5, 7, 10, 15, and 25 after DSS administration or day 0 by cardiac puncture under anesthesia and on days 0 and 10 from IL-6-deficient mice. The serum was separated by centrifugation and stored at −30°C until used for ELISA analysis.

Cell Culture

The human colonic adenocarcinoma COLO205 cell line was obtained from the American Type Culture Collection (ATCC, Manassas, VA). Cells were maintained in RPMI 1640 medium supplemented with 10% fetal bovine serum (FBS) (HyClone Laboratories, Logan, UT) and 1% penicillin–streptomycin (Nacalai Tesque) at 37°C under a humidified atmosphere of 5% CO_2.

For the analysis of LRG protein induction, COLO205 cells were stimulated with various concentrations of cytokines for 24 hours and culture supernatant were concentrated using Amicon Ultra-4 10K MWCO (Millipore, Bedford, MA). Concentrated supernatants were used for western blot analysis. Full-length human LRG cDNA was inserted into pcDNA3.1/V5-His-TOPO vector (Invitrogen) and designated pcDNA3.1-LRG-V5-His. pcDNA3.1-LRG-V5-His vector was transfected

into COS7 cells using Lipofectamine 2000 reagent (Invitrogen) and culture medium were used for the positive control.

Quantitative Real-time Reverse-transcription Polymerase Chain Reaction (RT-PCR) Analysis

For the quantification of mRNA levels of LRG, various mouse organs were analyzed by real-time RT-PCR as described previously.[23] Levels of mouse LRG and mouse hypoxanthine phosphoribosyltransferase (HPRT) levels were determined by the 7900HT Real-time PCR system (Applied Biosystems, Foster City, CA) using specific primers: murine LRG forward 5′-ATCAAGGAAGCCTCCAGGAT-3′; reverse 5′-CAGCTGCGTCAGGTTGG-3′ and murine hypoxanitine phosphoribosyltransferase (HPRT) forward 5′-TCAGTCAACG GGGGACATAAA-3′; reverse 5′-GGGGCTGTACTGCTT AACCAG-3′.

Statistics

The Mann–Whitney *U*-test or one-way analysis of variance (ANOVA) followed by a Scheffe's test were used for statistical analyses. Two-tailed Student's *t*-test was used for significant differences in LRG expression between identical patients with UC in active and remission disease stage. One-way ANOVA followed by a Dunnett's test was used for multiple comparison of the difference of serum LRG levels at various timepoints after DSS treatment in mice. Pearson's test was used to analyze the relationship between LRG and CRP, IL-6, or CAI. For drawing of receiver operating characteristic (ROC) curves and estimation of the area under the ROC curve (AUC) statistics, the software Excel Statistics 2010 (Social Survey Research Information, Tokyo, Japan) was used to quantify the ability to differentiate between remission and active by CAI. $P < 0.05$ was considered significant.

Ethical Considerations

Informed consent was obtained from all donors and all studies involving human subjects were approved by the Institutional Review Boards of the National Institute of Biomedical Innovation, Osaka University Hospital, the Department of Surgery, Osaka Rosai Hospital, and the University of North Carolina.

RESULTS

Serum LRG Levels Are Increased in Active UC Patients

We quantified serum LRG concentrations by ELISA using sera from patients with UC. Serum LRG concentrations were significantly elevated in the active UC patients (CAI ≥6) (14.24 ± 8.08 μg/mL) compared with HC (3.07 ± 1.42 μg/mL; $P < 0.0001$) (Fig. 1A). There was also a significant difference between LRG serum levels in patients with active UC (CAI ≥6) (14.24 ± 8.08 μg/mL) compared with UC in remission (CAI <6) (5.34 ± 2.60 μg/mL; $P <$ 0.0001) (Fig. 1A). To determine whether serum LRG levels are increased in non-IBD disease controls, we quantified serum LRG levels in patients with appendicitis and

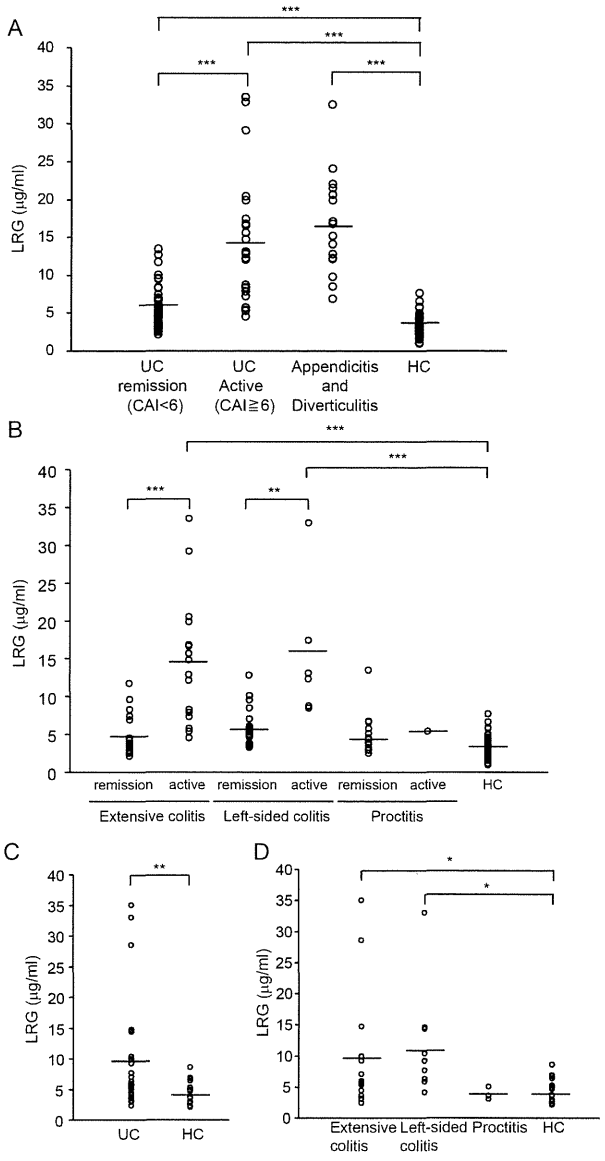

FIGURE 1. Serum LRG levels are increased in patients with active UC. (A) Serum levels of LRG were determined in 82 patients with UC (57 patients in remission [CAI <6], 25 patients in active [CAI ≥6] stage), appendicitis ($n = 13$), diverticulitis ($n = 4$) and 50 healthy controls (HC). ***$P < 0.0001$ by one-way ANOVA followed by Scheffe's post-hoc test. (B) Disease extension in UC was grouped into three categories: In UC patients in remission, extensive colitis ($n = 19$), left-sided colitis ($n = 24$), and proctitis ($n = 14$); in active patients, extensive colitis ($n = 18$), left-sided colitis ($n = 6$), and proctitis ($n = 1$) and HC ($n = 50$). **$P < 0.005$, ***$P < 0.0001$ by one-way ANOVA followed by Scheffe's post-hoc test. (C) Serum levels of LRG were determined in patients with UC ($n = 30$) and HC ($n = 19$) in a Caucasian cohort. **$P < 0.005$ by Mann–Whitney *U*-test. (D) In a Caucasian cohort, disease extension in UC was grouped into three categories: extensive colitis ($n = 16$), left-sided colitis ($n = 11$), and proctitis ($n = 3$) and HC ($n = 19$). *$P < 0.05$ by one-way ANOVA followed by Scheffe's post-hoc test.

diverticulitis. Elevated serum LRG levels were also observed in appendicitis and diverticulitis (16.83 ± 6.50 μg/mL) compared with HC (3.07 ± 1.42 μg/mL; $P < 0.0001$) (Fig. 1A), suggesting that serum LRG levels are also increased in acute intestinal inflammation.

When UC were classified into three categories based on disease extent, significantly higher serum LRG concentrations were observed in active patients with extensive colitis (14.34 ± 7.89 μg/mL) compared with in remission (4.96 ± 2.68 μg/mL; $P < 0.0001$) and HC (3.07 ±1.42 μg/mL; $P < 0.0001$) and active patients with left-sided colitis (15.41 ± 9.16 μg/mL) compared with in remission (5.91 ± 2.41 μg/mL; $P = 0.0003$) and HC (3.07 ±1.42 μg/mL; $P = 0.001$) (Fig. 1B). Nonetheless, there was no clear difference between active patients with proctitis and HC, possibly due to the low number of patients in this group. In patients with UC in remission, serum LRG levels in all of three disease extent categories were comparable with HC (Fig. 1B). Significantly elevated serum LRG levels were also detected in a Caucasian UC cohort (9.46 ± 8.44 μg/mL) compared with HC (4.42 ± 1.91 μg/mL; $P < 0.005$) (Fig. 1C). In this Caucasian UC cohort, serum LRG levels were also significantly elevated in patients with extensive colitis (9.54 ± 8.05 μg/mL) compared with HC (4.42 ± 1.91 μg/mL; $P < 0.05$) and left-sided colitis (10.90 ± 9.16 μg/mL) compared with HC (4.42 ± 1.91 μg/mL; $P < 0.02$) (Fig. 1D). However, a clear difference was not observed between patients with proctitis and HC (Fig. 1D). These results suggest that serum LRG levels were elevated in active UC.

Serum LRG Levels Are Correlated with Disease Activity in UC Patients

We investigated the correlation between serum LRG levels and disease activity (CAI) in UC patients. A positive correlation was observed between LRG and CAI ($r = 0.731$, $P < 0.00001$) (Fig. 2A). This correlation was stronger than that observed between CRP and CAI ($r = 0.654$, $P < 0.00001$) (Fig. 2A). When patients with UC were classified into active and remission according to the endoscopic findings, significantly elevated serum LRG levels and CRP levels were observed in patients with active UC compared with patients in remission ($P < 0.005$, respectively) (Supporting Fig. 1A). While serum LRG levels were significantly correlated with CRP levels in patients with UC ($r = 0.850$, $P < 0.00001$, $n = 82$) (Supporting Fig. 2A), such a correlation was not found when a CRP-negative subgroup (CRP <0.2, $n = 51$) was analyzed ($r = 0.101$, $P = 0.481$) (Supporting Fig. 2B). In this CRP-negative group, serum LRG levels were significantly correlated with CAI ($r = 0.416$, $P = 0.00241$) (Supporting Fig. 2C); however, significant correlation was not found between CRP and CAI ($r = -0.0896$, $P = 0.532$) (Supporting Fig. 2D). Additionally, in the CRP-negative group elevated serum LRG levels were detected in patients with endoscopically active UC compared with patients with UC in remission ($P = 0.0442$) (Supporting Fig. 1B). These findings in patients with low CRP may explain a better correlation of CAI with LRG than that with CRP.

When UC was classified by disease extent, a significantly higher positive correlation was detected between LRG and CAI than CRP and CAI both in extensive colitis ($r = 0.690$, $P < 0.000001$ and $r = 0.580$, $P = 0.000168$) and left-sided colitis ($r = 0.840$, $P < 0.000001$ and $r = 0.759$, $P < 0.000001$), but not in proctitis (Fig. 2B). Importantly, by analyzing sera obtained at active (CAI ≥6) and remission (CAI <6) disease stages from 10 identical UC patients, a significant decrease in serum LRG levels in remission was detected (Fig. 2C).

By generating an ROC curve, the sensitivity and specificity of serum LRG for remission and active by CAI were determined (Fig. 2D). The AUC for serum LRG levels was 0.901, whereas the AUC for CRP levels was 0.845. The cutoff value of serum LRG levels was 7.21 μg/mL (sensitivity = 84.0%, specificity = 82.5%). In contrast, when the cutoff value of CRP levels was set to 0.20, a maximum CRP value of normal range, the sensitivity was 80.0% and the specificity was 80.7%. These results emphasize the usefulness of monitoring serum LRG levels for the evaluation of the disease activity of UC.

Expression of LRG Was Increased in Inflamed UC Colons

Next, to investigate whether local inflammatory sites in patients with UC are a potential source of increased serum LRG we first looked at the expression of LRG in the colon by western blot analysis on inflamed and noninflamed sites of surgically resected full-thickness colon specimens from patients with UC. Western blot analysis showed that LRG expression in colon tissues was increased in inflamed sites of active UC patients compared with noninflamed colon tissues (Fig. 3A). Next, we tried to examine the localization of LRG. By immunohistochemistry, increased expression of LRG was detected in the cytoplasm of intestinal epithelial cells (IECs) in inflamed tissues (Fig. 3B–E). In contrast, expression of LRG was lower in noninflamed tissues (Fig. 3B–E). These data suggest that inflamed colon tissue is a potential source of increased serum LRG in patients with UC.

LRG Is Induced by Stimulation with TNF-α, IL-6, or IL-22

It has been reported that IL-6 is an inducer of LRG expression.[16] However, it is not clear whether LRG is induced by cytokines other than IL-6. At first we investigated the serum levels of IL-6, IL-22, and TNF-α, known

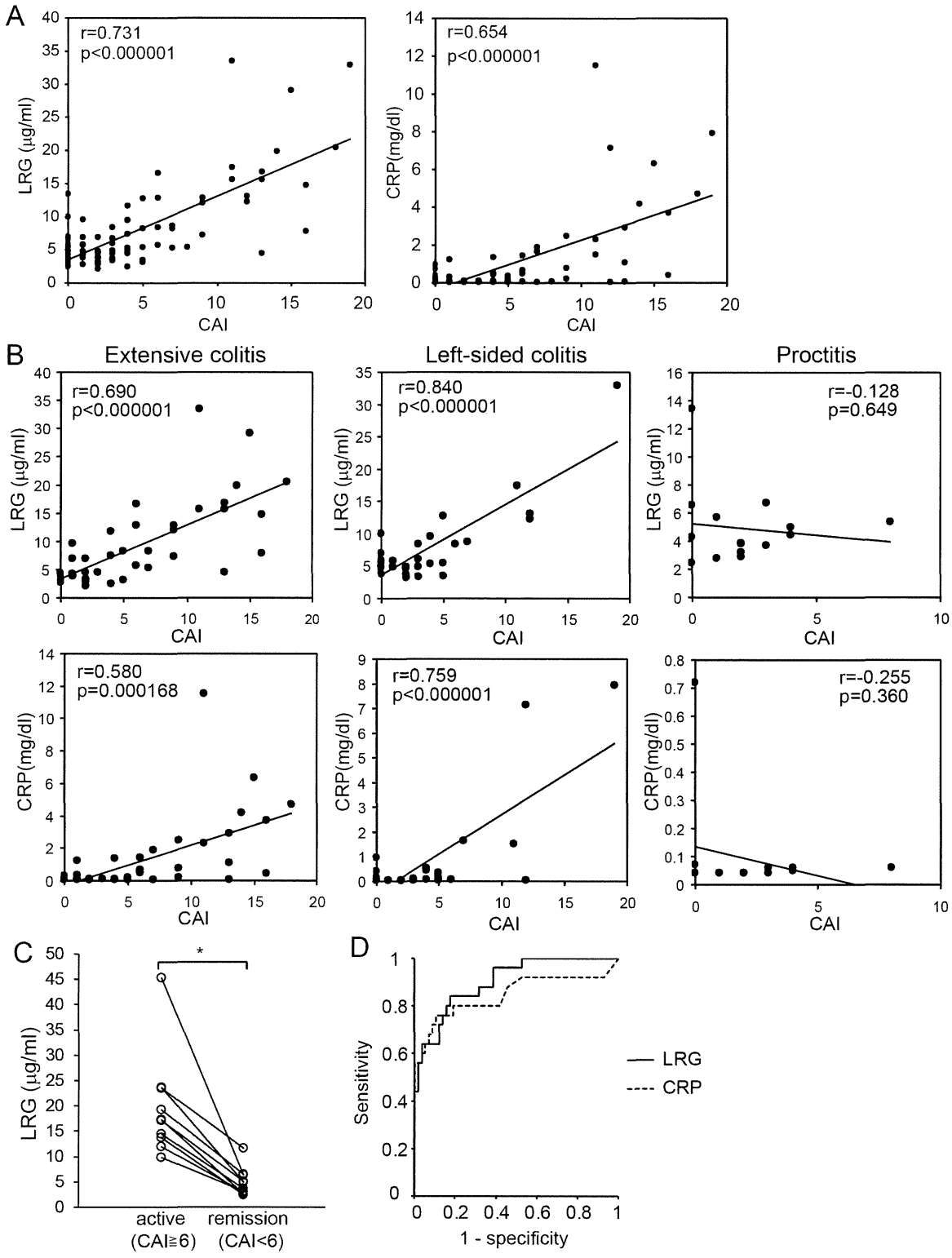

FIGURE 2. Serum LRG levels are correlated with disease activity better than CRP in patients with UC. (A) Serum levels of LRG correlated with CAI ($n = 82$; $P < 0.000001$; $r = 0.731$) better than CRP ($n = 82$; $P < 0.000001$; $r = 0.654$) in patients with UC. (B) Serum levels of LRG correlated with disease activity in extensive colitis ($n = 37$; $P < 0.000001$; $r = 0.690$) and left-sided colitis ($n = 30$; $P < 0.000001$; $r = 0.840$) better than CRP in extensive colitis ($n = 37$; $P = 0.000168$; $r = 0.580$) and left-sided colitis ($n = 30$; $P < 0.000001$; $r = 0.759$), while neither LRG ($n = 15$; $P = 0.649$; $r = -0.128$) nor CRP levels ($n = 15$; $P = 0.360$; $r = -0.255$) were correlated with disease activity in proctitis. (C) Compared with 10 identical active patients with UC, serum levels of LRG were decreased in remission. *$P < 0.002$ by Student's t-test. (D) ROC curves for LRG and CRP for differentiation between UC patients with remission ($n = 57$) and active ($n = 25$) by CAI.

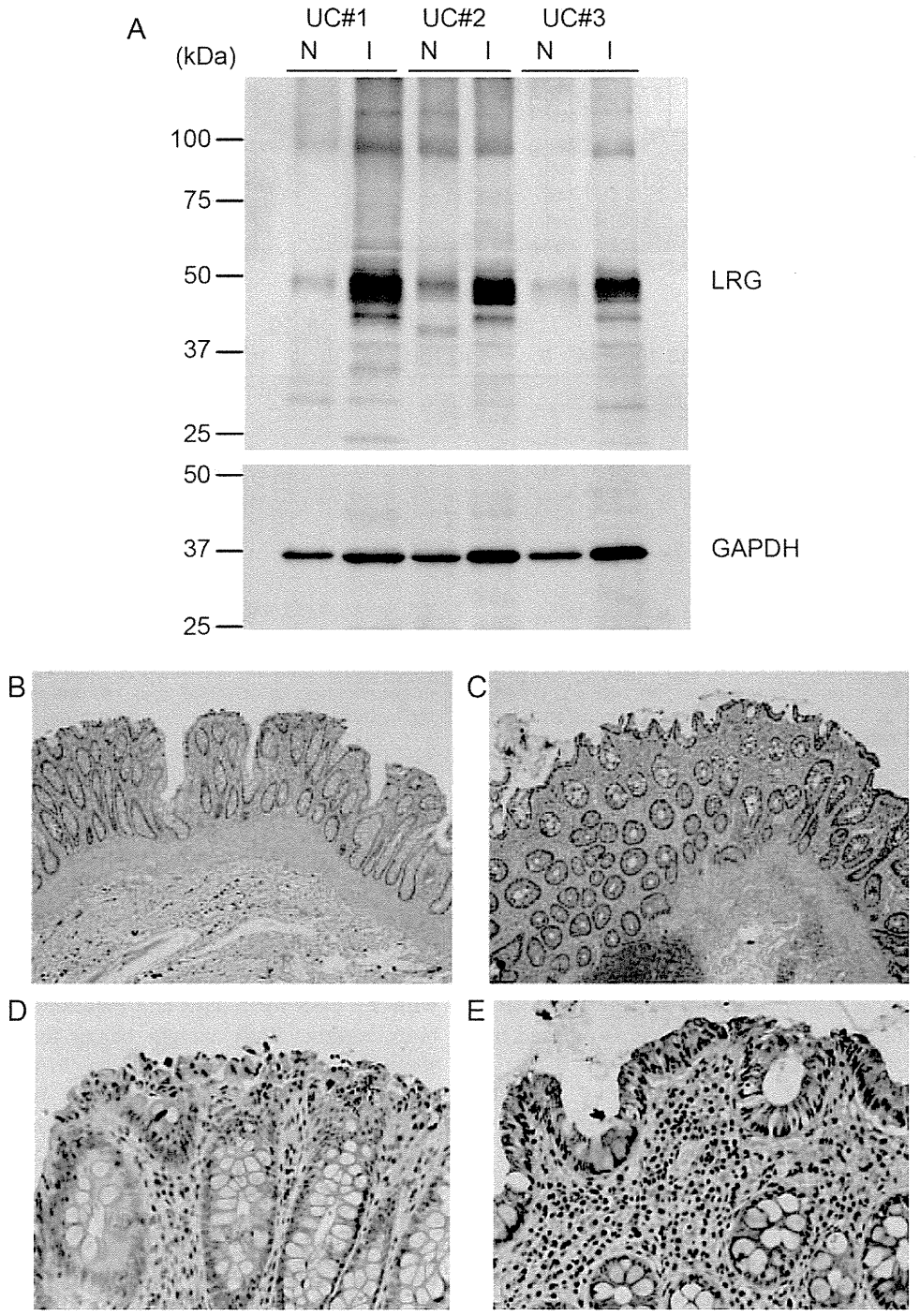

FIGURE 3. Expression of LRG is increased in lesion sites of ulcerative colitis. (A) Representative western blot analysis of three separate experiments for LRG using paired surgically resected full-thickness colon specimens from noninflamed (N) and inflamed (I) sites in patients with UC. GAPDH was used as a control of the relative amounts of proteins in each sample. Full-thickness colon tissues from UC in inflamed and noninflamed sites were evaluated by immunohistochemical analysis for LRG expression (n = 10 per experimental group). (B) Noninflamed mucosa (×42). (C) Inflamed mucosa from active UC (×42). (D) Noninflamed mucosa (×400). (E) Inflamed mucosa from active UC (×400).

to be increased at the inflamed tissue in active UC.[24–26] Indeed, ELISA analysis using sera from 82 UC patients revealed that serum TNF-α, IL-6, and IL-22 levels were significantly elevated in active UC patients compared with those patients in remission (P = 0.0178, P = 0.00690, and P < 0.0001, respectively) (Fig. 4A). Next, to investigate

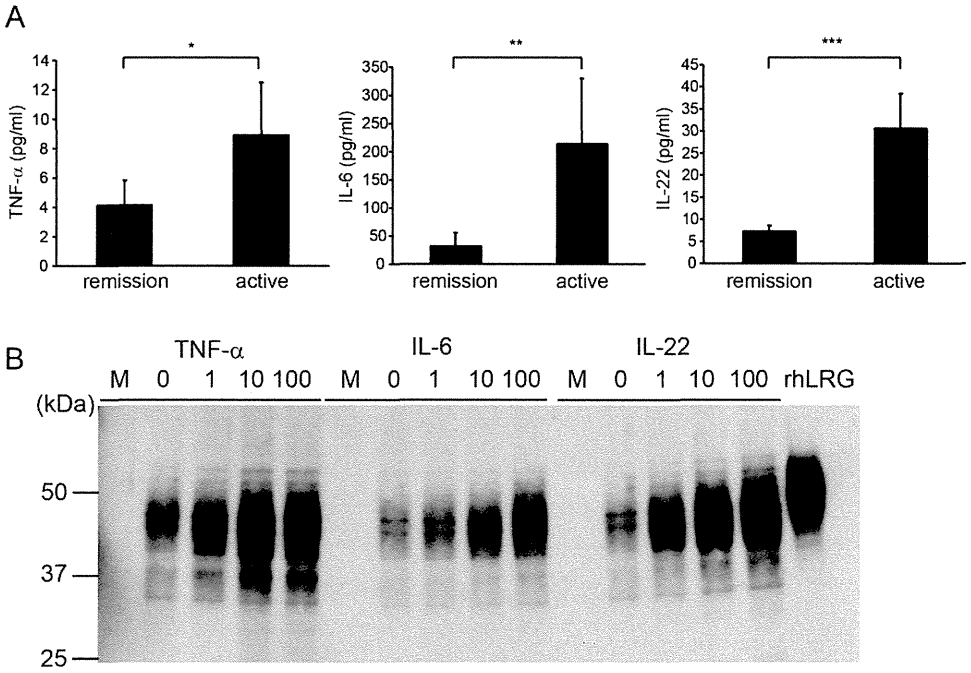

FIGURE 4. Expression of LRG was induced by TNF-α, IL-6, and IL-22. (A) Serum levels of TNF-α, IL-6, and IL-22 were determined in patients with UC (57 patients in remission [CAI <6] and 25 patients in active [CAI ≥6] stage). Data are expressed as mean ± SEM. *$P < 0.05$, **$P < 0.005$, ***$P < 0.0001$ by Mann–Whitney U-test. (B) LRG was determined in supernatants of COLO205 cells left untreated or stimulated with TNF-α, IL-6, and IL-22 at 1.0, 10, 100 ng/mL for 24 hours and analyzed by western blotting. There was a dose-dependent increase in LRG levels after treatment with TNF-α, IL-6, and IL-22.

which proinflammatory cytokines induce expression of LRG we stimulated human colonic adenocarcinoma COLO205 cells with TNF-α, IL-6, or IL-22 for 24 hours. After cytokine stimulation, secretion of LRG protein into the culture media was analyzed by western blotting. Interestingly, LRG was induced not only by stimulation with IL-6, but also by TNF-α and IL-22 in a dose-dependent manner (Fig. 4B). These results indicate that expression of LRG is induced by various proinflammatory cytokines including IL-6.

Expression of LRG Through an IL-6-independent Pathway Is Demonstrated in LPS-mediated Acute Inflammation and DSS-induced Colitis

CRP is one of the representative acute phase proteins in humans and CRP production is primarily dependent on liver by circulating IL-6. To examine the possible differences in induction mechanisms between LRG and CRP, particularly with regard to the involvement of IL-6, we took advantage of murine models. We first assessed whether LRG is induced in WT mice by injecting LPS, an inducer of proinflammatory cytokines from macrophages, because CRP is poorly induced in mice during acute inflammation. At 24 hours after intraperitoneal injection of LPS, serum samples were prepared and serum LRG levels were determined by ELISA. Compared with WT mice, significant elevation of serum LRG levels were detected in LPS-administered WT mice (Fig. 5A), suggesting that LRG is induced during acute inflammation in mice as in humans.

We next used a murine IBD model to investigate induction mechanisms of LRG during colonic inflammation. DSS-induced colitis is often used as a murine model of UC.[27] We induced colitis in WT mice by treating them with 3% DSS for 5 days and measured changes in relative body weight. Body weight began to decrease at day 5, showed greatest reduction at day 9, and recovered at 18 days after DSS treatment (Fig. 5B). We analyzed changes in serum LRG levels by ELISA before and 5, 7, 10, 15, and 25 days after DSS treatment. Consistent with body weight loss, serum LRG levels were significantly elevated at 5 days after DSS treatment (Fig. 5C). Serum LRG levels remained high until day 15, but decreased at day 25. Delayed normalization of serum LRG levels is likely due to the prolonged inflammation at inflamed tissue sites. Additionally, a long half-life of serum LRG might also be involved in this, since our preliminary data suggest that the half-life of serum human LRG levels are about two times longer than that of CRP (data not shown). To investigate which organs produce LRG in DSS-induced colitis, RNA was extracted from colon, liver, and spleen before and 9 days after DSS treatment. By quantitative PCR analysis (Fig. 5D), expression of LRG was significantly increased in liver ($P = 0.00106$) and spleen ($P = 0.0376$);

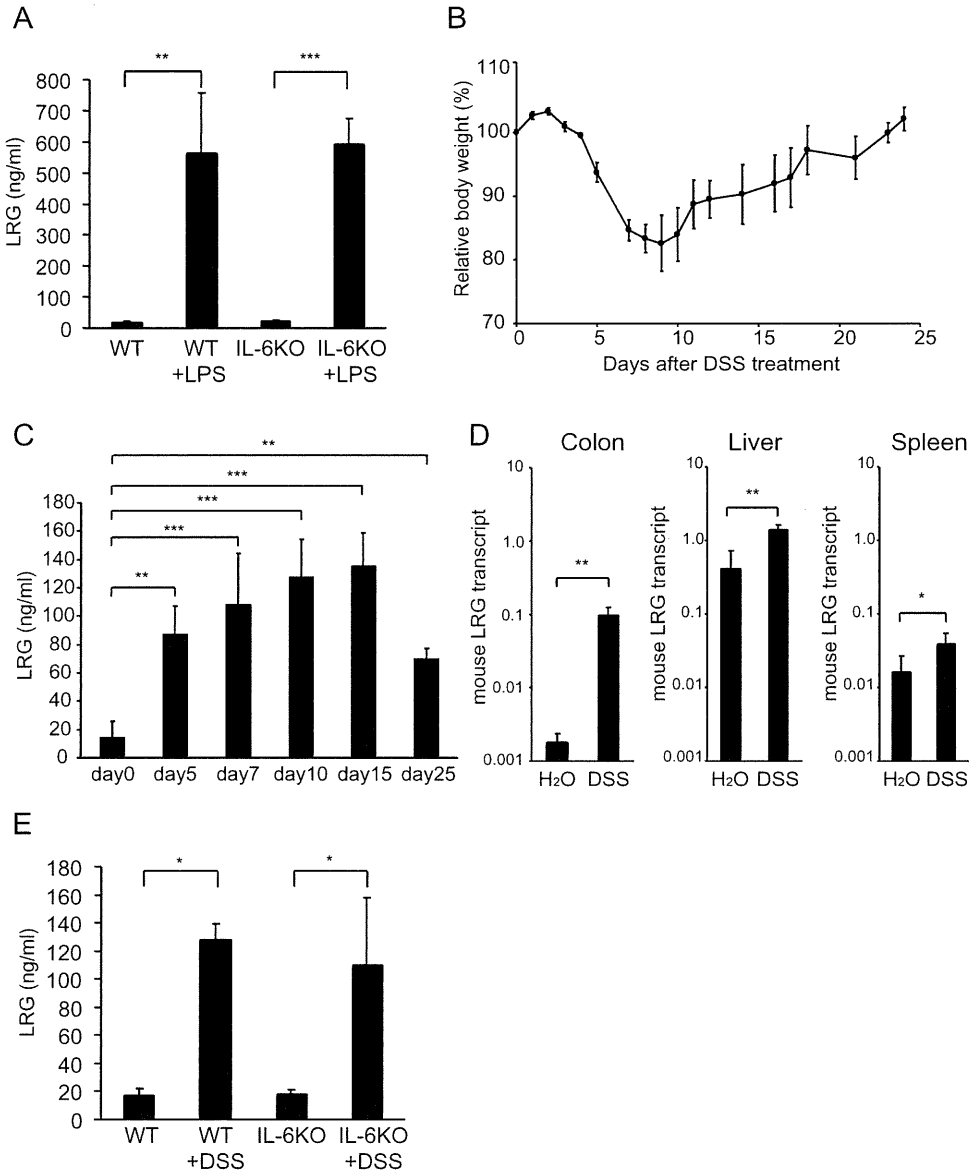

FIGURE 5. Induction of LRG has IL-6-independent pathway in LPS-mediated acute inflammation and active stage of DSS-induced colitis. (A) WT mice and IL-6-deficient mice were injected intraperitoneally with 0 or 10 mg/kg LPS dissolved in 500 μL PBS and serum LRG levels were measured after 24 hours. Data are expressed as mean ± SEM. $^{**}P < 0.005$, $^{***}P < 0.0001$ by one-way ANOVA followed by Scheffe's post-hoc test. (B) Relative body weight changes of mice with DSS-induced colitis in this study. Data are expressed as mean ± SEM ($n = 4$). (C) Expression of LRG is upregulated in murine DSS-induced colitis. At the indicated time, serum LRG levels were determined by ELISA analysis. $^{**}P < 0.005$, $^{***}P < 0.0001$ by one-way ANOVA followed by a by Dunnett's post-hoc test. (D) Nine days after control or DSS treatment, mice were euthanized and gene expression of LRG in the colon, liver, spleen, and kidney was determined by quantitative PCR analysis. Gene expression was calculated relative to HPRT. Data were expressed as mean ± SD ($n = 5$). $^{*}P < 0.05$, $^{**}P < 0.005$ by Student's t-test. (E) IL-6-deficient mice were used for DSS-induced colitis. Nine days after DSS administration, serum levels of mouse LRG was determined by ELISA analysis. $^{*}P < 0.05$ by one-way ANOVA followed by Scheffe's post-hoc test.

however, the strongest induction was observed in colon ($P = 0.000126$).

To investigate whether LRG induction is dependent on IL-6 or not, we analyzed serum LRG levels in IL-6-deficient mice. Interestingly, basal LRG levels in IL-6-deficient mice were similar to those in WT mice and LRG was robustly induced by LPS administration in IL-6-deficient mice (Fig. 5A). Moreover, increased serum LRG levels were also detected in the active stage (day 9) of DSS-induced colitis in IL-6-deficient mice (Fig. 5E). Importantly, the increase of serum LRG in IL-6-deficient mice was similar to that in WT mice (Fig. 5A,E). These findings indicate that LRG expression can be induced in the absence of IL-6.

DISCUSSION

In this study we first demonstrated that serum LRG levels were significantly increased in sera of active UC patients compared with patients in remission and HC. Serum LRG is likely elevated in diverse racial groups, because we detected increased serum LRG levels not only in Japanese patients (Fig. 1A)[13] but also in Caucasian patients with UC (Fig. 1C,D) and CD (data not shown). In addition, levels of serum LRG were significantly correlated with disease activity in UC and the correlation was stronger than CRP. Moreover, by analyzing ROC curve and AUC, serum LRG levels showed higher AUC than CRP and serum LRG levels represented superior sensitivity and specificity to CRP for remission and active of UC by CAI (Fig. 2D), indicating that LRG is a useful marker to evaluate disease activity in UC. In the normal state, serum LRG is thought to be produced from liver and LRG is abundantly found in the sera of HC. In colonic inflammation, we found that the expression of LRG is increased in the inflamed mucosa of UC patients and mice with DSS colitis, suggesting that inflamed tissues can be a source for production of LRG (Fig. 3). The increased expression of LRG in inflamed tissue has previously been observed in appendix during acute appendicitis.[28] Moreover, in acute inflammatory disorders, including appendicitis and diverticulitis, increased expression of serum LRG was observed (Fig. 1A). These results indicate that the elevated expression of LRG at inflamed sites and in sera occurs in various acute and chronic inflammatory disorders. Therefore, increased serum LRG levels are not suitable for use as a specific diagnostic marker of IBD.

CRP is the most common serum marker used to evaluate disease activity in inflammatory diseases. However, serum CRP is primarily dependent on liver production induced by circulating IL-6. Compared with CD and RA, only modest to absent CRP responses are observed in UC, despite active inflammation in colon.[9] Indeed, our cohort of 82 UC patients, analyzed in this study, included five patients with normal value of CRP while having active disease (Fig. 2A). However, our study demonstrated that serum LRG levels were significantly increased in active UC patients' sera and correlated better with disease activity of UC than CRP levels (Figs. 1A, 2A). Particularly, in the group of patients with negative CRP (CRP <0.2), significant correlation was observed between serum LRG levels and CAI (Supporting Fig. 2C). Similarly, among CRP-negative patients serum LRG levels were significantly elevated in those with endoscopically active UC, compared with UC in remission (Supporting Fig. 1B). In addition, serum LRG levels were decreased after therapy (Fig. 2C), suggesting that LRG is a useful serological biomarker for evaluating disease activity and therapeutic effect in UC.

Better correlation of serum LRG levels with disease activity of UC than CRP might be explained in part by the differences in induction mechanisms between LRG and CRP. While the expression of CRP is essentially dependent on IL-6, several cytokines may compensate for the absence of elevated IL-6 in induction of LRG expression. Accordingly, expression of LRG in COLO205 cells was induced not only by IL-6 but also by TNF-α and IL-22 (Fig. 4B), all of which were increased in sera of UC patients (Fig. 4A). Expression of LRG was strongly induced by IL-22 in COLO205 cells, correlating with enhanced STAT3 (Tyr705) phosphorylation by IL-22 compared with IL-6 (data not shown). Thus, inflammatory cytokines such as TNF-α and IL-22 may mediate LRG expression in the absence of IL-6. Moreover, using DSS-induced colitis in IL-6-deficient mice we could demonstrate an IL-6-independent pathway for LRG induction (Fig. 5E). Because promoter regions of human and mouse LRG share high sequence homology and contain putative binding sites for transcription factors such as C/EBP, MZF1, and STAT,[17] it is conceivable that the similar IL-6-independent mechanisms of LRG induction are also involved in humans. Future studies are required to fully elucidate the induction mechanisms of LRG in both humans and mice.

In the three disease categories of UC based on extent of disease, serum LRG levels tended to be low in proctitis compared with extensive colitis and left-sided colitis (Fig. 1B). In addition, correlation between serum LRG levels and disease activity did not reach significance in proctitis (Fig. 2B). Although the low number of patients with active proctitis may preclude the proper evaluation of LRG levels, limited inflamed area of proctitis may also be a reason for slight increases of serum LRG levels in these patients. Given the increased production of LRG in inflamed colonic mucosa, fecal LRG might be a more sensitive disease biomarker for UC including proctitis. Optimization for the measurement of fecal LRG is currently under way in our laboratory.

This study also highlights the potential usefulness of LRG in evaluating murine colitis. Our results indicate that serum LRG levels increase as the disease progresses in a DSS-induced colitis model (Fig. 5B,C). In addition, the LRG expression is significantly upregulated in the colon with DSS-induced colitis (Fig. 5D). Thus, LRG in mice can be an objective disease activity marker for colitis models and may be useful for preclinical studies of IBD.

In conclusion, serum LRG levels reflect disease activity of UC better than CRP, especially in patients with low CRP. In the inflammatory condition, LRG is expressed in the inflamed tissue and expression of LRG is regulated by mechanisms different from that of CRP. These findings suggest that serum LRG is a novel and potential serologic biomarker for evaluating disease activity of UC.

ACKNOWLEDGMENTS

We thank T. Mizushima for provision of appendicitis and diverticulitis patients' sera, Y. Kanazawa for secretarial

assistance, and M. Urase and A. Morimoto for technical assistance.

REFERENCES

1. Nikolaus S, Schreiber S. Diagnostics of inflammatory bowel disease. *Gastroenterology*. 2007;133:1670–1689.
2. Baumgart DC, Sandborn WJ. Inflammatory bowel disease: clinical aspects and established and evolving therapies. *Lancet*. 2007;369: 1641–1657.
3. Stange EF, Travis SP, Vermeire S, et al. European evidence based consensus on the diagnosis and management of Crohn's disease: definitions and diagnosis. *Gut*. 2006;55(Suppl 1):i1–15.
4. Caprilli R, Viscido A, Latella G. Current management of severe ulcerative colitis. *Nat Clin Pract Gastroenterol Hepatol*. 2007;4:92–101.
5. Kornbluth A, Sachar DB. Ulcerative colitis practice guidelines in adults (update): American College of Gastroenterology, Practice Parameters Committee. *Am J Gastroenterol*. 2004;99:1371–1385.
6. Sands BE, Abreu MT, Ferry GD, et al. Design issues and outcomes in IBD clinical trials. *Inflamm Bowel Dis*. 2005;11(Suppl 1):S22–28.
7. Freeman HJ. Use of the Crohn's disease activity index in clinical trials of biological agents. *World J Gastroenterol*. 2008;14:4127–4130.
8. Best WR, Becktel JM, Singleton JW, et al. Development of a Crohn's disease activity index. National Cooperative Crohn's Disease Study. *Gastroenterology*. 1976;70:439–444.
9. Vermeire S, Van Assche G, Rutgeerts P. C-reactive protein as a marker for inflammatory bowel disease. *Inflamm Bowel Dis*. 2004;10: 661–665.
10. Pepys MB, Druguet M, Klass HJ, et al. Immunological studies in inflammatory bowel disease. *Ciba Found Symp* 1977:283–304.
11. Saverymuttu SH, Hodgson HJ, Chadwick VS, et al. Differing acute phase responses in Crohn's disease and ulcerative colitis. *Gut*. 1986; 27:809–813.
12. Colombel JF, Rutgeerts P, Reinisch W, et al. Early mucosal healing with infliximab is associated with improved long-term clinical outcomes in ulcerative colitis. *Gastroenterology*. 2011;141:1194–1201.
13. Serada S, Fujimoto M, Ogata A, et al. iTRAQ-based proteomic identification of leucine-rich alpha-2 glycoprotein as a novel inflammatory biomarker in autoimmune diseases. *Ann Rheum Dis*. 2010;69:770–774.
14. Haupt H, Baudner S. Isolation and characterization of an unknown, leucine-rich 3.1-S-alpha2-glycoprotein from human serum [author's transl]. *Hoppe Seylers Z Physiol Chem*. 1977;358:639–646.
15. Takahashi N, Takahashi Y, Putnam FW. Periodicity of leucine and tandem repetition of a 24-amino acid segment in the primary structure of leucine-rich alpha 2-glycoprotein of human serum. *Proc Natl Acad Sci U S A*. 1985;82:1906–1910.
16. Shirai R, Hirano F, Ohkura N, et al. Up-regulation of the expression of leucine-rich alpha(2)-glycoprotein in hepatocytes by the mediators of acute-phase response. *Biochem Biophys Res Commun*. 2009;382: 776–769.
17. O'Donnell LC, Druhan LJ, Avalos BR. Molecular characterization and expression analysis of leucine-rich alpha2-glycoprotein, a novel marker of granulocytic differentiation. *J Leukoc Biol*. 2002;72: 478–485.
18. Rachmilewitz D. Coated mesalazine (5-aminosalicylic acid) versus sulphasalazine in the treatment of active ulcerative colitis: a randomised trial. *BMJ*. 1989;298:82–86.
19. Kruis W, Schreiber S, Theuer D, et al. Low dose balsalazide (1.5 g twice daily) and mesalazine (0.5 g three times daily) maintained remission of ulcerative colitis but high dose balsalazide (3.0 g twice daily) was superior in preventing relapses. *Gut*. 2001;49:783–789.
20. Matts SG. The value of rectal biopsy in the diagnosis of ulcerative colitis. *Q J Med*. 1961;30:393–407.
21. Iwahori K, Serada S, Fujimoto M, et al. Overexpression of SOCS3 exhibits preclinical antitumor activity against malignant pleural mesothelioma. *Int J Cancer*. 2011;129:1005–1017.
22. Kim A, Enomoto T, Serada S, et al. Enhanced expression of Annexin A4 in clear cell carcinoma of the ovary and its association with chemoresistance to carboplatin. *Int J Cancer*. 2009;125:2316–2322.
23. Fujimoto M, Nakano M, Terabe F, et al. The influence of excessive IL-6 production in vivo on the development and function of Foxp3+ regulatory T cells. *J Immunol*. 2011;186:32–40.
24. Murch SH, Lamkin VA, Savage MO, et al. Serum concentrations of tumour necrosis factor alpha in childhood chronic inflammatory bowel disease. *Gut*. 1991;32:913–917.
25. Woywodt A, Ludwig D, Neustock P, et al. Mucosal cytokine expression, cellular markers and adhesion molecules in inflammatory bowel disease. *Eur J Gastroenterol Hepatol*. 1999;11:267–276.
26. Andoh A, Zhang Z, Inatomi O, et al. Interleukin-22, a member of the IL-10 subfamily, induces inflammatory responses in colonic subepithelial myofibroblasts. *Gastroenterology*. 2005;129:969–984.
27. Okayasu I, Hatakeyama S, Yamada M, et al. A novel method in the induction of reliable experimental acute and chronic ulcerative colitis in mice. *Gastroenterology*. 1990;98:694–702.
28. Kentsis A, Lin YY, Kurek K, et al. Discovery and validation of urine markers of acute pediatric appendicitis using high-accuracy mass spectrometry. *Ann Emerg Med*. 2010;55:62–70 e4.

Tumor Biol. (2012) 33:1141–1149
DOI 10.1007/s13277-012-0356-9

RESEARCH ARTICLE

Serum HE4 as a diagnostic and prognostic marker for lung cancer

Kota Iwahori · Hidekazu Suzuki · Yoshiro Kishi · Yoshihiro Fujii · Rie Uehara · Norio Okamoto · Masashi Kobayashi · Tomonori Hirashima · Ichiro Kawase · Tetsuji Naka

Received: 19 December 2011 / Accepted: 9 February 2012 / Published online: 29 February 2012
© International Society of Oncology and BioMarkers (ISOBM) 2012

Abstract We evaluated the diagnostic and prognostic efficacy of human epididymis protein 4 (HE4) for lung cancer patients by using our novel enzyme-linked immunosorbent assay (ELISA) system. We measured serum HE4 levels of cancer patients including 49 lung cancer and 18 ovarian cancer patients. Furthermore, we evaluated the relationship between serum HE4 levels and overall survival after chemotherapy of 24 lung cancer patients. Serum HE4 levels were significantly higher for non-small, small cell lung cancer and ovarian cancer patients than for healthy controls. The area under the receiver operating characteristic curve (AUC) was calculated for differentiation of lung cancer patients and healthy controls. AUC for serum HE4 was 0.988 for differentiating lung cancer patients from healthy controls, with a cutoff value of 6.56 ng/ml (sensitivity= 89.8%, specificity=100%). Serum HE4 levels were elevated in 36/40 (90.0%) non-small cell lung cancer patients, 8/9 (88.9%) small cell lung cancer patients and 8/18 (44.4%) ovarian cancer patients. High levels of serum HE4 (>15 ng/ml) after chemotherapy were significantly correlated with worse overall survival after the treatment. These findings suggest that serum HE4 is a potential diagnostic and prognostic marker for lung cancer patients.

Keywords HE4 · Tumor marker · ELISA · Lung cancer · Chemotherapy

K. Iwahori · T. Naka (✉)
Laboratory for Immune Signal,
National Institute of Biomedical Innovation,
7-6-8 Saito-Asagi,
Ibaraki, Osaka 567-0085, Japan
e-mail: tnaka@nibio.go.jp

K. Iwahori
Department of Respiratory Medicine, Allergy, and Rheumatic Diseases, Osaka University Graduate School of Medicine,
2-2 Yamada-oka,
Suita, Osaka 565-0871, Japan

H. Suzuki · N. Okamoto · M. Kobayashi · T. Hirashima · I. Kawase
Department of Thoracic Malignancy, Osaka Prefectural Medical Center for Respiratory and Allergic Diseases,
3-7-1 Habikino,
Habikino, Osaka 583-8588, Japan

Y. Kishi · Y. Fujii · R. Uehara
Medical & Biological Laboratories, Co., Ltd.,
4-5-3, Sakae, Naka-ku,
Nagoya 460-0008, Japan

Introduction

Lung cancer is the leading cause of death in adult men in Europe, the United States, and Japan. In 2010, approximately 157,300 Americans died of lung cancer from among 569,490 cancer deaths [1]. The exceptionally high mortality rate of lung cancer is, in part, due to the fact that lung cancer is often diagnosed at a late stage when the prognosis is usually poor, and early detection continues to be an elusive goal. For patients with advanced stage disease, modest but real improvements in overall survival and quality of life have been achieved with systemic chemotherapy [2]. However, the determination of efficacy of chemotherapy during the early phase of treatment is difficult to achieve. The decision whether to continue or to stop chemotherapy is traditionally guided by imaging-based tumor response evaluation, which is regarded as a surrogate marker of clinical benefit. Assessment by structural imaging has known limitations and also may have a poor correlation with pathologic response in non-small cell lung cancer [3]. On the other

hand, tumor markers that are currently available for lung cancer such as carcinoembryonic antigen (CEA), serum cytokeratin 19 fragment (CYFRA 21-1) and progastrin-releasing peptide (pro-GRP) are not satisfactory for diagnosis at an early stage or for monitoring the disease because of their relatively low sensitivity and specificity in detecting the presence of cancer cells [4–6]. Therefore, the identification of novel diagnostic and prognostic biomarkers for treatment response is eagerly desired.

Human epididymis protein 4 (HE4) was first identified in the epithelium of the distal epididymis and originally predicted to be a protease inhibitor involved in sperm maturation [7, 8]. Regarding malignant neoplasms, gene expression profiling studies have identified upregulation of HE4 in ovarian cancer [9–14], and several studies have shown HE4 protein expression in ovarian cancer, providing the opportunity for its application in histopathologic diagnosis [15–18]. Recent studies have revealed elevated HE4 protein levels in serum from ovarian cancer patients [19]. Moreover, HE4 protein expression was analyzed in other neoplasms including lung cancer [20, 21]. In this study, we developed novel enzyme-linked immunosorbent assay (ELISA) system to detect serum HE4, and by using this system, we showed that HE4 has potential for diagnostic marker of lung cancer. Specifically, we found that HE4 level after chemotherapy is strongly correlated with survival after the treatment.

Materials and methods

Patients and controls for measurement of HE4

Serum samples were collected from 49 consecutive patients with lung cancer (33 with adenocarcinoma, six with squamous cell carcinoma, one with large cell carcinoma and nine with small cell carcinoma), 18 with ovarian cancer, 10 with gastric cancer and eight with colon cancer. For control, we used 37 healthy adults (Table 1). The age range in 37 healthy control subjects was between 24 and 65 years. The age range in 49 lung cancer patients was between 40 and 78 years. We obtained written and oral informed consent from all participants. This study was approved by our institutional review board (IRB).

Patients for evaluation of chemotherapy

This prospective, IRB-approved study included 24 patients enrolled between 28 April 2008 and 26 August 2008. Patient characteristics are presented in Table 2. The median age was 69 years (45–76 years). All patients received chemotherapies. Specific regimens are presented in Table 2. Computed tomography (CT) scans were performed after 2 cycles of chemotherapy or 1 month of gefitinib/erlotnib therapy. All patients had measurable disease. Response categories were defined according to the Response Evaluation Criteria in Solid Tumors (RECIST) as complete response (CR), partial response (PR), stable disease (SD) and progressive disease (PD).

Cell lines

Nonsmall cell lung cancer cell lines A549, NCI-H1793, LU61, PC14, PC14PE6, PC9, SKLU1 and SKMES2; breast cancer cell line MCF7; colon cancer cell lines LOVO and WiDr; gastric cancer cell lines GC1Y, GT3TKB, HGC27, KATO3, MKN45 and OCUM1; pancreatic cancer cell line Miapaca2; prostate cancer cell lines 22Rv1 and PC3; and bladder cancer cell line T24 were cultured in DMEM medium (Sigma, St Louis, MO) supplemented with 10% fetal bovine serum (Equitech Bio Inc., Kerrville, TX). Non-small cell lung cancer cell line A427 was cultured in E-MEM medium (Sigma) supplemented with 10% fetal bovine serum. Non-small cell lung cancer cell lines NCI-H226, NCI-H358, NCI-H520, NCI-H522, NCI-H596, NCI-H2170, LC174, LC319 and ChagoK1; small cell lung cancer cell line DMS114; gastric cancer cell lines SCH, MKN74 and MKN1; pancreatic cancer cell lines KLM1, PK59 and PK1; and breast cancer cell line T47D were cultured in RPMI (Sigma) supplemented with 10% fetal bovine serum.

Table 1 Serum concentrations of HE4 in cancer patients and controls

Diagnosis	Number of study participants	HE4 (ng/ml)			Positive ratio (%)
		Mean (SD)	Median	Range	(Cutoff 6.56 ng/ml)
Lung cancer	49	14.0 (9.5)	11.4	4.3–63.4	89.8
NSCLC	40	13.3 (6.5)	11.4	4.3–30.7	90.0
SCLC	9	17.3 (18.1)	11.4	5.5–63.4	88.9
Ovarian cancer	18	10.9 (13.6)	6.1	2.0–60.2	44.4
Gastric cancer	10	7.2 (4.4)	7.1	2.1–17.4	60.0
Colorectal cancer	8	7.7 (3.5)	7.1	3.0–12.2	62.5
Normal	37	2.7 (1.2)	2.4	1.3–5.8	

Table 2 Patient characteristics

Characteristics	Number of patients
Gender	
Males/females	16/8
Age (years)	
<71/>71	13/11
Stage	
3A/3B/4	4/5/15
Tumor histology	
Adenocarcinoma	15
Squamous	4
Unclassified NSCLC	1
Small	4
Chemotherapy	
NSCLC	
Carboplatin + paclitaxel	5
Vinorelbine	3
Irinotecan	3
Cisplatin + gemcitabine	2
Gefitinib	2
Erlotinib	2
Carboplatin + gemcitabine	1
Cisplatin + vinorelbine	1
Gemcitabine	1
SCLC	
Carboplatin + etoposide	2
Cisplatin + etoposide	1
Cisplatin + irinotecan	1
Clinical response	
NSCLC	
CR/PR/SD/PD	0/5/10/5
SCLC	
CR/PR/SD/PD	0/3/1/0

Culture supernatants were collected at 5 to 6 days after cultivation and stored at 4°C until test.

Antigen preparation

Recombinant human HE4 protein was produced by amplifying the part coding for amino acids 1–124 from the cDNA encoding the transcript for human HE4 (Genbank accession no. NM_006103) with DNA polymerase (recombinant Taq polymerase; Takara Bio Inc., Shiga, Japan) and using the primers 5′-CGGGATCCGAGAAGACTGGCGTGTGCCCCG-3′ and 5′-TTTAAAGCGGCCGCTCAGAAATTGGGAGTGACA CAGG-3′. The amplified DNA was inserted into the *Bam*HI/*Not*I site of a mammalian expression plasmid DNA vector pSecTag2/Myc-His (Invitrogen, Carlsbad, CA) and transfected into HEK 293 T cells by lipofection (Lipofectamine 2000; Invitrogen). The culture supernatant of the transfectant was recovered at 5 days after lipofection and applied to a TALON resin to purify the secreted His-tagged proteins according to the manufacturer's instructions (Takara). The purified HE4 protein thus obtained was dialyzed with 4.0 l of PBS twice and kept frozen at −80°C until use as an immunogen or as a standard polypeptide for sandwich ELISA. Purity of the recombinant HE4 was confirmed by Coomassie Brilliant Blue (CBB) staining after electrophoresis under reduced condition (Fig. 1a).

Membrane-bound form of HE4 was constructed by molecular fusion together with the transmembrane region of a type I cell surface protein HIDE1 (accession number: A8MVS5) as briefly described below. Membrane-bound form of HE4 was produced by amplifying the part coding for amino acids 1–125 and 114–164 from the cDNAs of HE4 gene and HIDE1 gene, respectively, and both amplified DNAs were inserted into the *Xba*I site of pcDNA3.1/myc-His. *IRES-GFP* gene (Cell Biolabs, Inc., San Diego, CA) was then inserted into the *Pme*I site of the same plasmid DNA. The plasmid DNA was transfected into HEK 293 T cells, and GFP-positive cells were accounted for the cells expressing membrane bounded HE4.

Immunogen to develop a polyclonal antibody to human HE4 was prepared as follows. The part coding for amino acids 31–124 of the HE4 cDNA was ligated to the *Eco*RI/*Xho*I site of a bacterial expression vector pET28a (Novagen, Madison, WI). BL21 (DE3) competent cell (Takara) was transformed with the pET28a plasmid and cultured in LB medium. After induction of expression of HE4 protein using IPTG, the bacteria was collected and lysed with PBS containing 8 M urea, 1% NP-40, 0.5 mM PMSF and protease inhibitor cocktail (Sigma, St. Louis, MO). After centrifugation at 13,000*g* for 15 min, the supernatant containing His-tagged HE4 protein was loaded on a TALON resin, and the recombinant HE4 was eluted from the resin with 200 mM imidazole solution according to the manufacturer's instructions (Takara).

Antibody generation

To generate monoclonal antibodies against human HE4, 4-week-old BALB/c mice were immunized intraperitoneally with the recombinant HE4 produced from 293 T transfectant on days 0, 7, 14 and 16 (10 μg/shot). Following the last immunization, lymphocytes of the spleen were collected and fused with P3U1 myeloma cells in a 50% polyethylene glycol 4000 solution (Wako, Osaka, Japan) on day 18. The fused cells were plated on 96-well plates with RPMI-1640 medium containing 15% fetal calf serum (Equitech-Bio), penicillin/streptomycin (Invitrogen, Carlsbad, CA) and HAT solution (Invitrogen). After 10 days of incubation at 37°C with 5% CO_2 in a humidified environment, culture supernatants were collected and screened for their ability to bind to the immunogen by ELISA using recombinant HE4. Selected positive hybridoma colonies were expanded and

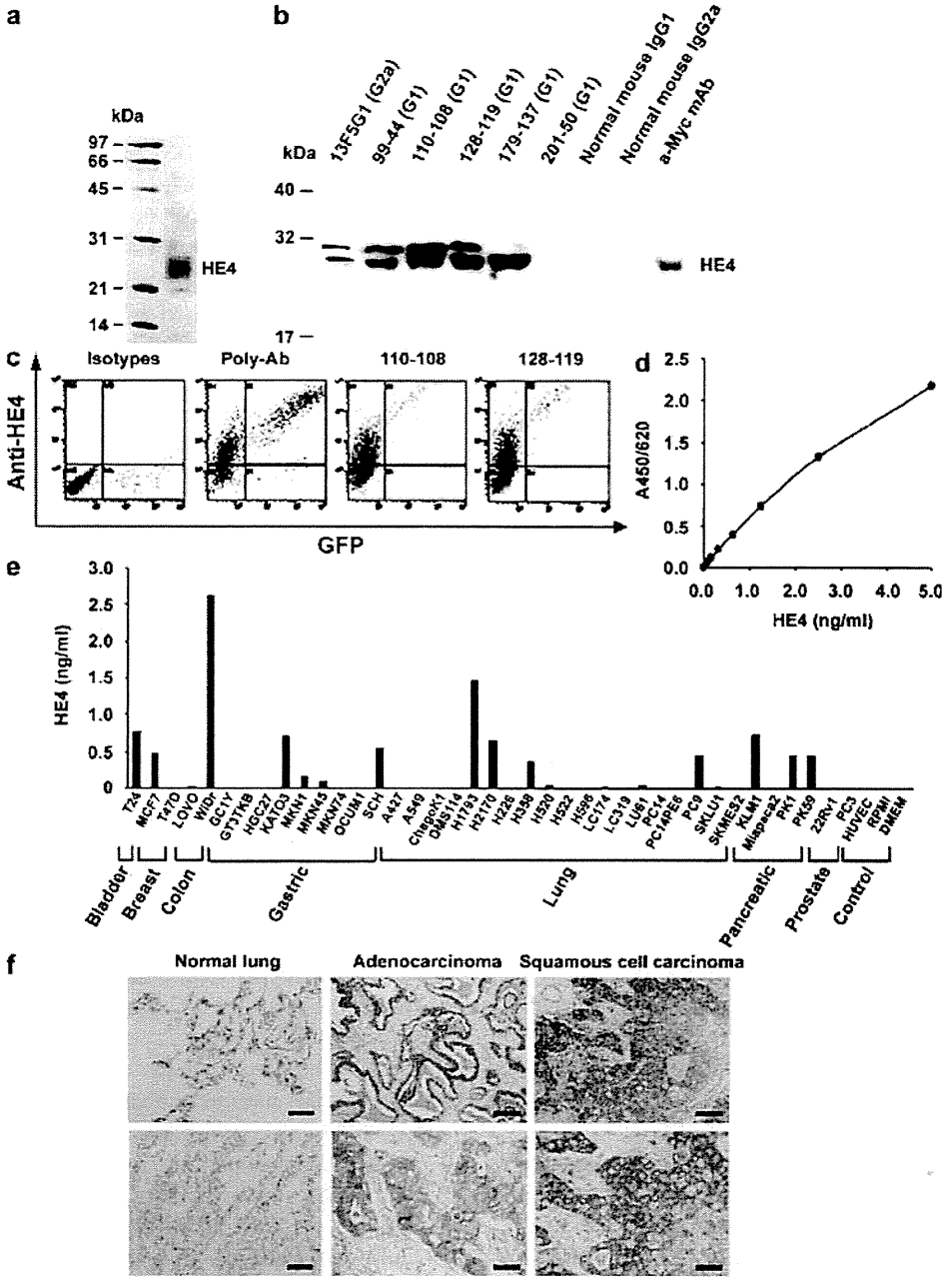

Fig. 1 **a** Purity of the prepared recombinant HE4 proteins for immunization. Proteins were electrophoresed under reduced condition and stained with Coomassie Brilliant Blue. **b** Reactivity of anti-HE4 antibodies to recombinant HE4 protein. Anti-HE4 antibodies were used for immunoprecipitation. Recovered proteins were separated by SDS-PAGE and electrotransferred to polyvinylidenefluoride (PVDF) membranes. Membranes were probed with anti-myc antibody for myc-His tagged HE4. Recombinant HE4 protein was applied for positive control. **c** Expression of HE4 on the surface of HE4-transfected 293 T cells. 293 T cells were incubated with anti-HE4 antibodies (110-108 and 128-119) or an isotype-matched control antibody and followed by PE-conjugate anti mouse IgG. Antigen expression was detected by flow cytometry. **d** Standard curves for HE4 in sandwich ELISA. ELISA displaying the mean absorbance values from indicated concentrations of recombinant proteins. **e** HE4 levels in the supernatants of cell lines measured by specific ELISA systems. **f** Immunohistochemical analysis of HE4 in lung cancer tissue. *Scale bar upper panels* 100 μm, *scale bar lower panels* 50 μm

subcloned by limiting dilution. An isostrip kit (Hoffmann-La Roche, Basel, Switzerland) was used for antibody isotype determination according to the manufacturer's instructions. Antibody purification was carried out with protein A affinity chromatography (GE Healthcare, Buckinghamshire, UK). Following a competition assay for the immunogen among the clones thus obtained (data not shown), clone 110-108 (IgG1) and clone 128-119 (IgG1) were selected to construct a sandwich ELISA for the detection of HE4.

Polyclonal antibody to recombinant human HE4 was prepared by injecting Japanese white rabbits (Kitayama Labs, Nagano, Japan) with purified HE4 (100 μg/injection) from *E. coli* subcutaneously in complete Freund's adjuvant followed by subsequent boosts in incomplete Freund's (Sigma). The serum was collected and IgG-purified with Protein G Sepharose (GE Healthcare).

Flow cytometry

At 24 h after transfection of the plasmid DNA-encoding membrane-binding HE4 into 293 T cells, the transfectant was treated with PBS containing 5 mM EDTA for 3 min to